uOttawa

L'Université canadienne
Canada's university

FACULTÉ DES ÉTUDES SUPÉRIEURES ET POSTOCTORALES

uOttawa

L'Université canadienne
Canada's university

FACULTY OF GRADUATE AND POSDOCTORAL STUDIES

Alexandre Ibrahim
AUTEUR DE LA THÈSE / AUTHOR OF THESIS

M.Sc. (Earth Science)
GRADE / DEGREE

Department of Earth Sciences
FACULTÉ, ÉCOLE, DÉPARTEMENT / FACULTY, SCHOOL, DEPARTMENT

Biogeochemical Mapping of Bacteriogenic Iron Oxide in a Freshwater Wetland in Chalk River, Ontario, Canada
TITRE DE LA THÈSE / TITLE OF THESIS

Danielle Fortin
DIRECTEUR (DIRECTRICE) DE LA THÈSE / THESIS SUPERVISOR

CO-DIRECTEUR (CO-DIRECTRICE) DE LA THÈSE / THESIS CO-SUPERVISOR

J. Blais

F. Michel

Gary W. Slater
Le Doyen de la Faculte des etudes superieures et postdoctorales / Dean of the Faculty of Graduate and Postdoctoral Studies

Biogeochemical mapping of bacteriogenic iron oxides in a freshwater wetland at Chalk River, Ontario, Canada

Alexandre Ibrahim

Thesis submitted to the Faculty of Graduate and Postdoctoral Studies, University of Ottawa, in partial fulfillment of the requirements for the M.Sc. degree in the Earth Sciences

Ottawa-Carleton Geoscience Centre

and

University of Ottawa

Ottawa, Canada

Your file Votre référence
ISBN: 978-0-494-73787-3
Our file Notre référence
ISBN: 978-0-494-73787-3

Table of Contents

List of Figures v

List of Tables vi

Résumé vii

Abstract viii

Acknowledgements ix

1. Introduction 1

1.1 Formation and occurrence of BIOS 1

1.1.1 Chemical and microbial Fe(II)-oxidation 1

1.1.2 Hydrolysis and precipitation of BIOS 3

1.1.3 Mineralogy of BIOS 4

1.2 BIOS in the environment 5

1.2.1 Sorption properties of BIOS 5

1.2.2 Redox stability of BIOS 7

1.3 Background on project 8

1.4 Objectives and hypotheses 10

2. Materials and methods 12

2.1 Study site 12

2.1.1 Site description 12

2.1.2 Sampling sites 13

2.2 Aqueous geochemistry 14

2.2.1 Physical chemistry 14
2.2.2 Dissolved cations and anions 14
2.2.3 Dissolved inorganic and organic carbon 15
2.3 Solid phase biogeochemistry 15
2.3.1 Morphology 15
2.3.2 Mineralogy 15
2.3.3 Crystallinity and bioavailability of Fe 16
2.4 Statistical analyses 16
2.4.1 Geochemical correlations 16
2.4.2 Predictors of DIC 16

3. Results 18
3.1 Aqueous geochemistry 18
3.1.1 Physical chemistry 18
3.1.2 Geochemistry 19
3.1.3 Geochemical correlations 20
3.1.4 Predictors of DIC 20
3.2 Solid phase biogeochemistry 21
3.2.1 Morphology 21
3.2.2 Mineralogy 21
3.2.3 Crystallinity and bioavailability of Fe 22

4. Discussion 23

4.1 Solid phase biogeochemistry 23

4.1.1 BIOS occurrence and morphology 23

4.1.2 BIOS mineralogy 24

4.1.3 BIOS crystallinity and bioavailability of Fe 26

4.2 Aqueous geochemistry 27

4.2.1 Spatial variations 27

4.2.2 Sources and cycles of Fe and DIC 30

4.2.3 Geochemical interactions 32

5. Conclusions 34

6. Environmental implications 36

References 37

Appendix A 57

Appendix B 58

List of Figures

Figure 1. Scanning electron micrographs of iron oxidizing bacteria 42
associated with iron oxides

Figure 2. Map of Ontario, Canada with the location of Chalk River with 42
respect to Ottawa and Toronto

Figure 3. Regional map (Google Earth image) of the location of the study site 43
with respect to the recharge zone (Lake 233) and the general
groundwater flow path (blue arrow) of the area

Figure 4. Seasonal photographs taken at site CR01 44

Figure 5. Map with the location of the 11 sampling sites within the 45
wetland boundaries

Figure 6. Spatial variations of the physicochemical and geochemical parameter 46

Figure 7. Seasonal X-ray diffraction patterns of surface BIOS 47
and BIOS-free sediments

List of Tables

Table 1. Physicochemical parameters of the surface water in the wetland 48

Table 2. Chemical composition of the surface water in the wetland 51

Table 3. Spearman rank correlation coefficients of the physicochemical 54
and geochemical parameters

Table 4. Multiple regression analysis used to determine significant predictors 55
of DIC

Table 5. Seasonal chemical extraction of solid phase Fe in BIOS 56

Résumé

Des accumulations importantes d'oxydes de fer biogéniques (BIOS) se forment près d'une source d'eau souterraine riche en Fe(II) dissout dans un marais arboré (superficie d'environ 12 000 m^2) situé à Chalk River, Ontario, Canada. Les BIOS possèdent des caractéristiques qui peuvent potentiellement servir à la séquestration des contaminants, tels que les métaux lourds (e.g, Sr^{2+} et potentiellement aussi des isotopes radioactives, $^{90}Sr^{2+}$, $^{129}I^-$ and ^{14}C), présents dans les eaux souterraines. Cette thèse a fait l'étude des propriétés biogéochimiques (aqueuses et solides) des BIOS formant dans le marais. Les résultats des études minéralogiques ont démontré que les BIOS se composent principalement de ferrihydrite à deux lignes et de petites quantités de lépidocrocite. La phase minérale de goethite a aussi été identifiée en quantité minime dans les échantillons de BIOS prélevés durant les mois les plus chauds de l'année pour deux des sites étudiés. La cristallinité du Fe solide réactif, compris dans les BIOS, augmente en aval des zones de déchargements d'eaux souterraines dans le marais, alors que la biodisponibilité du Fe diminue. Les analyses géochimiques de l'eau de surface du marais ont révélé une corrélation importante entre le Fe(II) dissout et le carbone inorganique dissoute (CID) (r_s = 0.83). Ces deux paramètres sont soupçonnés de faire part d'un cycle biogéochimique complexe, surtout dans un environnement riche en BIOS. Le Fe(II) dissout et le CID sont soit consommés par la chimiosynthèse utilisée par les bactéries durant la formation des BIOS, *ou soit, produits pendant la réduction microbienne des oxydes de Fe(III) qui est couplée avec l'oxydation de la matière organique.* Ces données serviront à mieux comprendre la stabilité des BIOS à long terme dans un environnement naturel.

Abstract

Large accumulations of bacteriogenic iron oxides (BIOS) form near Fe(II)-rich groundwater springs in a freshwater wetland located at Chalk River, Ontario, Canada, covering an area of approximately 12 000 m^2. BIOS are efficient sorbent and may potentially serve as an *in situ* bioremediation method to sequester contaminants, such as heavy metals (e.g. Sr^{2+} and potentially radioisotopes, $^{90}Sr^{2+}$, $^{129}I^-$ and ^{14}C), present in the groundwater. This study focused on the aqueous geochemistry of the wetland, as well as, the solid phase biogeochemistry of BIOS sediments. The mineralogy of BIOS was mainly composed of poorly ordered 2-line ferrihydrite, with minor amounts of lepidocrocite. Goethite was also detected in sediment samples collected during the warmer seasons at two of the sites. Crystallinity of the reactive solid phase Fe in BIOS increased downstream (approx. 10m) from groundwater discharge areas, whereas, Fe(III) became less bioavailable. Analyses of surface water sampling revealed that dissolved Fe(II) and dissolved inorganic carbon (DIC) were significantly correlated (r_s = 0.83). These two parameters are thought to be involved in a complex biogeochemical cycling in BIOS-rich environments. Both, dissolved Fe(II) and DIC are consumed by chemosynthesis used by iron-oxidizing bacteria during the formation of BIOS or produced during the microbial reduction dissolution of Fe(III)-oxides coupled with the oxidation of organic matter. These results provided valuable information concerning the long term redox stability of BIOS in the natural environment.

Acknowledgements

I would like to thank my family for their moral and financial support throughout my academic years. Without them I would have never come this far and would not have eaten so well during my field trips.

I also wish to thank my 'bestest' supervisors ever, Danielle Fortin and Grant Ferris. You have both taught me and guided me through this challenging, yet interesting part of my life. I appreciate the opportunity you gave me in pursing this research (Ph.D next? Maybe!) I also thank you for offering me to work in collaboration with the Deep River Science Academy, who assigned 5 high school students to work on my project. This was a valuable experience.

To my 'peeps', Sean and Andy (Team BIOS), it would not have been the same experience without you (holding back tears). Thanks to all my other fellow lab partners and undergraduates who helped us. Special thanks to Doug and Shelagh Ogilvie who have always accommodated us with great hospitality for the past several years. And they fed me good too!

1. Introduction

1.1 Formation and occurrence of BIOS

Bacteriogenic iron oxides (BIOS) are comprised of naturally occurring iron oxides[1] that are formed and precipitated directly onto or in proximity to bacterial cells and extracellular substances, forming macroscopic aggregates in the environment (Ferris, 2005; Fortin and Langley, 2005). BIOS can form and occur in a wide range of environments if the physical and chemical conditions are appropriate; i.e., a continuous source of dissolved ferrous iron (Fe(II)), circumneutral pH conditions, micro-aerobic conditions (low pO_2), slow water flow rate and presence of iron-oxidizing bacteria (FeOB). The different types of environments where BIOS have been known to form and occur include freshwater wetlands (James and Ferris, 2004; Emerson and Weiss, 2004; Duckworth et al., 2009), hydrothermal sea vents (Kennedy et al., 2003; Edwards et al., 2003; Langley et al., 2009a), subsurface environments (Anderson et al., 2006) and on the rhizosphere of wetland plants (Emerson et al., 1999; Weiss et al., 2007).

1.1.1 Chemical and microbial Fe(II)-oxidation

The formation of BIOS results from the chemical and microbial oxidation of dissolved Fe(II) and usually occurs in sub-oxic environments where the anoxic Fe(II)-rich groundwater is discharged to the surface. The interaction between the anoxic groundwater and the oxygenated environment, at groundwater discharge areas, leads to the rapid oxidation of Fe^{2+} to Fe^{3+} catalyzed by both chemical and microbial processes:

[1] The term iron oxides refers to all Fe(III)-bearing oxides, hydroxides and oxyhydroxides.

$$4\ Fe^{2+} + O_2 + 4\ H^+ \leftrightarrow 4\ Fe^{3+} + 2\ H_2O$$ **[1]**

At circumneutral pH, the chemical Fe^{2+}-oxidation rate is extremely fast in well-oxygenated environments, i.e., oxidation occurs within a matter of minutes (Stumm and Morgan, 1996; Neubauer et al., 2002). However, low concentrations of dissolved oxygen, typically observed in sub-oxic environments, tend to impede the chemical Fe^{2+}-oxidation rate to a point where the microbial Fe^{2+}-oxidation rate becomes the kinetically favoured reaction (Neubauer et al., 2002; James and Ferris, 2004). In circumneutral environments, the microbial oxidation reaction is accomplished by specialized neutrophilic iron-oxidizing bacteria (FeOB), such as *Gallionella ferruginea*, *Leptothrix ochracea* and *Sideroxydans paludicola* (Hallbeck and Pedersen, 1991, 2003; James and Ferris, 2004; Weiss et al., 2007). These species thrive mostly in environments characterized by low pO_2 and a continuous supply of circumneutral Fe(II)-rich groundwater. Under acidic conditions, the chemical Fe^{2+}-oxidation rate is usually extremely slow and iron oxidation is essentially driven by microbial activity, such as *Acidithiobacillus ferrooxidans*, which is an acidophilic FeOB (Baker and Banfield, 2003; Edwards et al., 2000) .

The role of the various FeOB in the formation of BIOS can be both the result of active or passive processes (Fortin and Langley, 2005). In the case of an active process, the FeOB ultimately gain energy from the transfer of electrons during the oxidation reaction of Fe^{2+} to Fe^{3+} and utilize the energy gained from the reaction to support their basic cellular functions. On the other hand, the passive processes refer to the fact that there are potential sites for mineral nucleation of iron oxide particles, such as bacterial cell walls and extracellular substances, including the helical stalks produced by *Gallionella ferruginea* or the tubular sheaths produced by *Leptothrix ochracea* (Fortin and Langley, 2005).

1.1.2 Hydrolysis and precipitation of BIOS

The chemical and microbial oxidation of dissolved Fe^{2+} is the first step in the formation of BIOS, whereas the second step consists of the hydrolysis of dissolved Fe^{3+}, as it reacts with water molecules:

$$Fe^{3+} + nH_2O \leftrightarrow Fe(OH)_n^{(3-n)+} + nH^+ \textbf{ [2]}$$

Under a continuous influx of dissolved Fe^{3+} into solution, there is an increase in the concentration of hydrolyzed species and consequently an increase of the ion activity product (IAP), i.e., the ratio of concentrations of dissolved Fe^{3+} to protons in solution. Once the IAP becomes greater than the solubility product of a specific mineral phase, the solution becomes oversaturated and nucleation and precipitation start to occur. However, the point of critical oversaturation must be reached before precipitation of any solids can occur (Warren and Ferris, 1998).

Microorganisms can also play a crucial role in the nucleation and precipitation of iron oxides by offering reactive cell surface sites (e.g. carboxyl and phosphoryl groups) that adsorb dissolved Fe^{3+}. Once all of the reactive cell surface sites have been completely saturated with Fe^{3+}, the solution will eventually become oversaturated with the additional influx of dissolved Fe^{3+}. In fact, the presence of bacteria is thought to reduce the point of critical oversaturation, therefore increasing the rate of precipitation of iron oxides when compared to abiotically formed oxides (Warren and Ferris, 1998; Ferris, 2005). Precipitation of nano-sized iron oxide particles mainly occurs along the bacterial cell walls as well as their extracellular structures,

such as the helical stalks and tubular sheaths of *Gallionella* and *Leptothrix* species, respectively (Fig. 1).

1.1.3 Mineralogy of BIOS

The bulk mineralogy of iron oxides is generally comprised of amorphous to poorly ordered 2-line ferrihydrite, as well as more crystalline phases such as lepidocrocite, goethite and hematite (Châtellier et al., 2004; Fortin and Langley, 2005). In general, iron oxides tend to occur as nano-sized particles with a highly heterogeneous surface reactivity and a high surface area to volume ratio (Cornell and Schwertmann, 2003). These characteristics are what make iron oxides efficient sorbents for a wide range of trace elements, including heavy metals and radionuclides (Fortin et al., 1993; Cornell and Schwertmann, 2003).

According to the Ostwald step rule, amorphous and poorly-ordered 2-line ferrihydrite are expected to be the first iron oxide phases to precipitate since they tend to be the most soluble of all iron oxide phases and thus, the most energetically favourable products to form (Stumm and Morgan, 1996). However, 2-line ferrihydrite is likely to undergo phase transformation towards more crystalline iron oxide phases via dissolution and re-precipitation reactions (as part of the aging process) (Cornell and Schwertmann, 2003). The precise phase towards which 2-line ferrihydrite is to transform is dependent on the environmental conditions, such as temperature (Kennedy et al., 2004), concentration of dissolved Fe(II) and concentrations of specific ligands, e.g., Cl^-, SO_4^{2-} and CO_3^{2-} (Hansel et al., 2003; Hansel et al., 2005). Under laboratory conditions, a study by Hansel et al. (2005) suggested that 2-line ferrihydrite can undergo complete phase transformation towards more crystalline phases, such

as lepidocrocite, goethite, magnetite and hematite. However, little information is known about the evolution of BIOS mineralogy in natural settings, e.g., a groundwater-supplied wetland that represents an open-system environment.

1.2 BIOS in the environment

BIOS have been suggested to act as efficient sorbents for nutrients and heavy metals (potentially radionuclides) (Ferris et al., 1999; Langley et al., 2009b). In fact, many corporate and governmental agencies (e.g. Atomic Energy of Canada Ltd (AECL)) have become increasingly interested in scientific research aimed at bioremediation methods that are cost-effective and require limited disturbance to the natural environment.

1.2.1 Sorption properties of BIOS

BIOS have become the focus of many studies in recent years due to their sorption efficiency to sequester heavy metals (e.g. Cd, Cs, Pb, U and Sr) (Ferris et al., 1999, Ferris et al., 2000, Langley et al., 2009b) and potentially radionuclides (e.g. $^{90}Sr^{2+}$, $^{129}I^{-}$ and ^{14}C) from contaminated groundwater. In fact, the two fractions of BIOS composites, i.e., the bacterial fraction (cells and exopolymers) and the mineral fraction (iron oxides), are what make BIOS such efficient sorbents in comparison to abiotically formed iron oxides. Both bacteria and iron oxides play a role in the sorption of trace elements due to their high surface reactivity. The bacterial cell wall is generally composed of numerous reactive cell surface sites that exhibit an overall net negative charge, making it an efficient sorption surface for positively charged metal ions under circumneutral pH conditions (Fein et al., 1997).

A study by Martinez et al. (2003) determined the proportion of selected metals that were either sorbed to the bacterial cell wall or to the oxide fraction of BIOS. They measured the concentrations of metals adsorbed to the iron oxide fraction by reacting the BIOS with hydroxylamine and then deducted the concentrations of metals adsorbed to the bacterial fraction from a total digestion of the BIOS. The results indicated that, in the solid phase, Al (69.5%), Cu (78.7%) and Zn (77.9%) were closely associated to the bacterial fraction of BIOS, whereas, Cr (59.8%), Mn (99.8) and Sr (79.4%) favoured the oxide fraction. This simply suggests that BIOS are highly heterogeneous and may adsorb a wide range of nutrients and contaminants.

A recent study (Langley et al., 2009b) suggested that the sorption of strontium onto BIOS was highest at low ionic strength (I = 0.001 M), while at higher ionic strength (I = 0.1 M), the sorption was significantly inhibited, indicating that Sr was sorbed as an outer-sphere complex, as confirmed by extended X-ray adsorption fine structure (EXAFS). In addition, strontium remained completely unbound at pH below 4.5 and reached a maximum sorption capacity at pH greater than 7.5. The sorption edge where 50% of the strontium was adsorbed to BIOS was determined to be at pH 6.06. Another recent study by Kennedy et al. (2010) revealed that BIOS was also an efficient sorbent for iodine (I). Field measurements at the AECL site at Chalk River, Ontario, showed that the waters in contact with BIOS had significantly lower levels of ^{129}I than BIOS-free sites. The above results suggest that BIOS is an efficient sorbent for contaminants, such as strontium and iodine in dilute and circumneutral wetlands.

1.2.2 Redox stability of BIOS

Although BIOS appear to be effective in the sequestration of contaminants from groundwater, they are also susceptible to reductive dissolution by iron-reducing bacteria (FeRB) at depth where anoxic conditions occur. If BIOS are reduced by FeRB, then the potential of contaminant re-mobilization into groundwater will effectively increase. Langley et al., (2009c) studied the reduction rates of natural BIOS and synthetic hydrous ferric oxide (HFO), as well as strontium desorption from these iron oxides. Reduction rates of BIOS with naturally low levels of strontium were significantly decreased when BIOS were loaded with strontium. Strontium loading of HFO did not exhibit the same effect, i.e., reduction rates were similar to those of strontium-free HFO. These findings suggest that BIOS would sequester strontium from highly contaminated environments. The authors also found that strontium was released (80 – 100%) during the reduction of BIOS and did not re-adsorb or co-precipitate with secondary minerals such as vivianite during their laboratory experiments (Langley et al., 2009c).

The fate of contaminants released during BIOS reduction will ultimately depend on the biogeochemical properties of the environment where they occur. It is difficult to predict the outcome of contaminants in the environments strictly based on experimental models that have pre-determined conditions (closed-system). In microaerophilic environments, such as groundwater springs, where the oxic and anoxic boundaries are relatively close, trace elements may potentially be involved in intense biogeochemical cycling. For instance, Fe(II) oxidized to Fe(III) at the surface will tend to precipitate as Fe(III)-oxides that are then prone to reductive dissolution thus, re-releasing Fe(II) into solution. Dissolved Fe(II) could then diffuse upwards, therefore regenerating the Fe cycle or precipitate as Fe(II)-bearing minerals at depth. The fate

and transport of contaminants may be directly influenced by Fe cycling, especially in environments where BIOS deposits form and occur (Langley et al., 2009b, c).

1.3 Background on project

The research conducted throughout this study was accomplished in partnership with Atomic Energy of Canada Limited (AECL) at the Chalk River Laboratories in Ontario, Canada. AECL has always been concerned about low-level radioactive contamination of the water supplies in proximity to their nuclear waste storage sites from which radionuclides, such as $^{90}Sr^{2+}$, $^{129}I^-$ and ^{14}C, which can leach into the groundwater. Human health concerns, primarily bone cancer, soft tissues cancers and leukemia have been linked to exposure to $^{90}Sr^{2+}$ that substitutes for Ca^{2+} in the human body (Nielsen, 2004). In recent years, there has been a lot of interest in using naturally occurring BIOS as a potential natural bioremediation approach for contaminated groundwater (Langley et al., 2009b).

Recent studies conducted under laboratory conditions have assessed the sorption properties of BIOS for strontium and iodine in order to extrapolate the results to their respective radionuclides, i.e., ^{90}Sr and ^{129}I (Langley et al., 2009b, Kennedy et al., 2010). Both studies showed excellent sorption characteristics for BIOS, but Langley et al. (2009c) reported that under reducing conditions and in the presence of an iron reducing bacterium, most of the sorbed strontium was released back into solution, along with Fe(II). These laboratory experiments suggest the potential remobilization of contaminants if there is a tight coupling of iron oxidation and reduction reactions in environments where BIOS form. The present study therefore investigates the biogeochemical parameters linked to BIOS formation and occurrence

in a specific wetland where copious amounts of BIOS naturally occur. Such study should yield a better representation of the actual biogeochemical processes controlling BIOS formation in natural settings.

Wetlands, particularly those that contain significant amounts of BIOS deposits, are known to play a pivotal role in the biogeochemical cycling of organic and inorganic matter including nutrients (e.g. Fe and C), contaminants and sediments (Ontario Wetland Evaluation System (OWES) Northern Manual, 2003). The sources, fate and transport of these nutrients, contaminants and sediments in the environment are dependent on natural factors, such as regional hydrogeology, geomorphology, vegetation patterns, as well as anthropogenic influences, such as agricultural and industrial activities. The biogeochemical processes, driven both chemically and biologically, occurring within wetlands often serve to regulate the quality of surface and ground water originating from upstream environments before being funnelled towards downstream effluents such as creeks, lakes, rivers and oceans.

Many wetlands in the Chalk River region, particularly on the AECL property, are supplied by circumneutral pH and anoxic groundwater rich in dissolved ferrous iron (Fe(II)) promoting the formation of BIOS at groundwater discharge areas. The proximity of the aerobic and anaerobic boundaries in micro-aerobic environments is expected to promote rapid cycling between the oxidation of dissolved Fe(II) and the reductive dissolution of solid phase Fe(III). While Fe is one of the most significant elements being cycled in such environments, the fate and transport of other nutrients and contaminants can be greatly affected. This is why BIOS have gained more attention in recent studies that examined their use as a potential in situ bioremediation technique to attenuate contaminated sites.

1.4 Objectives and hypotheses

The scope of this study was part of a broader project funded by the Natural Science and Engineering Research Council (NSERC) of Canada. Objectives from the NSERC project include the sorption properties of BIOS with respect to Sr^{2+} and I^- retention, susceptibility of BIOS to reductive dissolution and subsequent mobilization of Sr^{2+} and the sequestration and cycling of carbon in BIOS (potential immobilization of ^{14}C). Dr. Sean Langley, a former Ph.D student at the University of Ottawa, addressed the main objectives of the project i.e., microbial reduction rates of BIOS, sorption of Sr onto BIOS and desorption of Sr during BIOS reduction.

The overall objective of the current study was to assess the seasonal and spatial biogeochemistry of bacteriogenic iron oxides (BIOS) naturally occurring in a groundwater-supplied wetland located on the AECL property at Chalk River, Ontario. The study was subdivided into to two specific objectives:

1) To study the seasonal and spatial variations of the surface water geochemistry (with a focus on Fe and C) of the groundwater-supplied wetland in order to assess the role of BIOS in regulating the biogeochemical cycles of trace elements and contaminants. It was expected that significant variations in surface water geochemistry, particularly downstream of BIOS deposits would occur. If correlations between different geochemical parameters can be made, then it would provide better insight on the long term biogeochemistry of BIOS.

2) To study the solid phase biogeochemistry of BIOS, particularly their mineralogy, from various sampling locations (collected at various times of the year) within the

groundwater-supplied wetland at Chalk River, Ontario, Canada, where BIOS formed and occurred perennially. It was hypothesized that aging; i.e., transformation toward more crystalline phases of Fe(III)-oxides, would occur in BIOS as the iron oxide-bacteria aggregates were carried away from the point of groundwater discharge where they originally formed.

2. Materials and methods

2.1 Study site

2.1.1 Site description

The study site is a groundwater-supplied wetland located on the property of Atomic Energy of Canada Ltd. (AECL) in Chalk River, Ontario, approximately 180 km northwest of Ottawa, Ontario, Canada (Fig. 2). The wetland boundaries cover an area of approximately 25 000 m^2, but the scope of the present study covered close to half of the total area in order to focus mainly on sites where BIOS deposits occurred. The boundaries of the wetland were mapped using handheld GPS units following guidelines from the OWES Northern manual (2003), in which the wetland boundary is defined as the point where the vegetation comprises 50% wetland species and 50% upland species. Following the criteria of the OWES Northern manual (2003), the AECL wetland is deemed a coniferous forest swamp, predominated by *Thuja occidentalis* (American white cedar) with minor coverage of low wetland shrubs, with standing to low flowing water.

The wetland is situated at the base of a steep, 20 m-high sand dune that serves as an aquifer (10 ka aeolian deposits) for water recharge from a nearby freshwater lake (Lake 233) (Fig. 3). Along the base of the dune, several BIOS deposits are observed perennially where Fe(II)-rich anoxic groundwater discharges into the wetland (Fig. 4). The groundwater springs feed numerous streams throughout the wetland that flow at least 75 meters downstream, east of the sand dune. The streams eventually recharge back into the aquifer or discharge into downstream effluents beyond the boundaries of the wetland. Most of the fresh, flocculent BIOS form and occur nearest to Fe(II)-rich groundwater springs, whereas further downstream, the

stream sediments simply appeared to be coated with iron oxides. Also, precipitation and surface runoff serve an additional source of water to the wetland.

2.1.2 Sampling sites

Sampling took place in the spring (mid-April 2007 and late April 2008), summer (late July 2007), fall (mid-October 2007) and winter (early February 2008). A total of eleven sites were selected to represent the different dynamics of the wetland over a broad spatial scale (Fig. 5). Four sites (CR01, CR03, CR05 and CR10) were located most upstream of the wetland at less than a meter from the Fe(II)-rich groundwater springs. One site (CR02) was located midstream at approximately 10 m away from the groundwater spring. Four additional sites (CR06, CR07, CR08 and CR09) were located further downstream at more than 10 m from the groundwater springs within the streamlines of some upstream sites. In addition, two BIOS-free sites (i.e., no evidence of BIOS deposits at the surface), BF01 and BF02, were both located upstream at less than a meter from the groundwater springs, where concentrations of dissolved Fe were low or below limits of detection.

Fresh and flocculent BIOS deposits were observed perennially at sites CR01, CR02, CR03, CR05 and CR10, whereas, at sites CR06, CR07, CR08 and CR09, there was no presence of flocculent BIOS but rather significant amounts of iron oxide coatings on the sediments. There was no occurrence of BIOS at both BIOS-free sites, however, minor amounts of iron oxide coatings were observed on the sediments at site BF01 in the winter of 2008.

2.2 Aqueous geochemistry

2.2.1 Physical chemistry

Physicochemical parameters of surface water (i.e., pH, redox potential (Eh), temperature and concentration of dissolved oxygen (DO)) were measured *in situ* with a handheld data logger YSI 650MDS equipped with a multi-electrode probe YSI 600QS. The probe was calibrated before every sampling session and rinsed with ultrapure water (UPW) between each sampling site.

2.2.2 Dissolved cations and anions

Surface water samples were collected and dispensed into 50 ml acid washed polyethylene bottles using 20 ml sterile syringes. The samples were filtered (0.2 μm) and acidified on site to 0.02M HCl and stored at 4°C until analysis in the laboratory. Concentrations of dissolved cations (Al, Na, K, Ca, Mg, Si, Sr, Fe, Mn) were determined using a Varian Vista-Pro CCD simultaneous inductively-couple plasma – optical emission spectrometer (ICP-OES).

Sub-samples of acidified surface water samples were used to determine the concentrations of dissolved Fe(II) using the ferrozine assay (Stookey, 1972). Concentrations of dissolved Fe(III) were determined as the difference between the concentrations of total dissolved Fe and dissolved Fe(II).

Additional surface water samples were collected and filtered (0.02) in 50 ml acid washed polyethylene bottles using 20 ml sterile syringes and stored at 4°C until analysis in the laboratory. The samples were analyzed for major anions (Cl and SO_4) using an ion chromatograph (model Dionex DX-100).

2.2.3 Dissolved inorganic and organic carbon

Surface water samples were collected and dispensed in 40 ml amber glass vials using 20 mL sterile syringes and stored at 4°C until analysis in the laboratory. Concentration of dissolved inorganic (DIC) and organic (DOC) carbon, as well as the delta 13-C isotopic ratios ($^{13}C_{DIC}$ and $^{13}C_{DOC}$) were determined using an OI Analytical TIC-TOC analyzer (model 1010) interfaced to an isotope ratio mass spectrometer (DeltaPlus Advantage, ThermoFinnigan, Germany), as described by St-Jean (2003).

2.3 Solid phase biogeochemistry

2.3.1 Morphology

Scanning electron microscopy (SEM) of surface BIOS sediments collected in February 2007 at site CR01 were performed. Briefly, BIOS samples were washed 5 times in acetone and critical point dried (Balzers Intrusments, CPD010, Liechtenstein). The SEM images were obtained using a JEOL JSM-6301F Field Emission Gun Scanning Electron Microscope operated at 9 kV.

2.3.2 Mineralogy

Subsamples of surface BIOS and BIOS-free sediments were freeze-dried and ground to a fine powder using a mortar and pestle. The mineralogy of all samples was determined by powder X-ray diffraction (XRD) using a Philips PW 1830 X-ray diffractometer, with a Cu-Kα X-ray source, operating at 45 kV with a current of 40 mA. Continuous scans were run from 2 to 70° 2θ range using a step size of 0.02°, counting 6 s per step for the BIOS samples and 1 s per step for the BIOS-free sediment samples.

2.3.3 Crystallinity and bioavailability of Fe

Non-sequential solid phase extraction of reactive Fe(III) from surface BIOS and BIOS-free sediments were performed as described by Kostka and Luther (1994) to assess the crystallinity of the reactive iron in BIOS. Four chemical extractants were used for this study; HCl, ascorbate, oxalate and dithionite. The amount of Fe(III) extracted with ascorbate is considered to represent the bioavailable Fe that could be utilized by Fe(III)-reducing microorganisms (Hyacinthe et al., 2006). The amount extracted with HCl should reflect the bioavailable Fe as well as any Fe associated with acid volatile sulfides (AVS). The oxalate extractant is able to reduce more crystalline iron oxide phases, such as goethite, but not hematite. Dithionite, in return, extracts all reactive Fe(III) in the sediments including both amorphous and crystalline iron oxide mineral phases.

2.4 Statistical analyses

2.4.1 Geochemical correlations

The statistical analyses of the aqueous geochemical data were computed with Statistica 8.0 (Statsoft®). Non-parametric Spearman rank correlation (r_s) tables were generated to determine any significantly correlated geochemical parameters. Spearman rank correlation is widely used when the distribution of the data is non-Gaussian.

2.4.2 Predictors of DIC

Step-wise multiple linear regression analyses were conducted using a general linear model to determine predictors of DIC concentrations. The geochemical parameters that were

significantly correlated with DIC were computed in multiple regression analyses using DIC as the dependent variable. If a variable was found not to be a significant predictor of DIC, it was dropped from the model and the analysis was redone until all independent variable were statistically significant ($p < 0.05$). The model was accepted once a strong correlation ($R^2 > 0.90$) was obtained and that there was no evidence of multicollinearity between the independent variables.

3. Results

3.1 Aqueous geochemistry

3.1.1 Physical chemistry

The physicochemical measurements for are reported in Table 1. Surface water pH values remained in the circumneutral range (5.4 – 6.8) throughout the seasons, slightly increasing downstream of groundwater discharge areas (Fig. 6). Water temperatures (3.1 – 13.0°C) were warmest in the summer and coldest in the winter, likely reflecting changes in ambient air temperatures. Redox potential values were the highest in the winter at all BIOS sites, with the exception of site CR03 and the BIOS-free site. The redox potential measured at site CR03 was not at its highest during the winter, but the reported value was comparable to the other sites. Concentrations of dissolved oxygen were considerably lower in the summer and increased as a function of distance from the groundwater discharge springs. At the BIOS-free sites, the dissolved oxygen values were generally higher than those measured at the BIOS sites. An increase in degradation of organic matter during the warmer months was the likely cause of the decrease in concentrations of dissolved oxygen in the summer months, when the conditions were near-anoxic (if measurement errors are taken into consideration).

The partial pressure of CO_2 in the surface water was calculated (Table 1) using the following equations:

$$K_{CO_2} = \frac{a_{H_2CO_3}}{P_{CO_2}} = 10^{-1.47} \qquad [3]$$

$$K_1 = \frac{a_{HCO_3^-} \cdot a_{H^+}}{a_{H_2CO_3}} = 10^{-6.35} \quad [4]$$

It was assumed that the carbonate species did not contribute significantly to the total concentration of DIC since the pH of the wetland remained well below pH 8.4 (Stumm and Morgan, 1996).

3.1.2 Geochemistry

The complete geochemical data are reported in Table 2. Figure 6 shows the most prominent spatial trends observed in the wetland's aqueous geochemistry. Values for pH, dissolved oxygen concentrations and isotopic fractionation of inorganic carbon (delta $^{13}C_{DIC}$) were the lowest near the groundwater springs and increased downstream inversely to the spatial trends observed for dissolved Fe(II) and DIC concentrations. Dissolved Fe(III) concentrations showed little spatial variations in the wetland and remained relatively low when compared to concentrations of dissolved Fe(II). At the control sites, concentrations of dissolved Fe were consistently low or below the detection limit, never exceeding 2.86 µM.

Redox potential and dissolved Fe(III) concentrations measured at sites (CR01, 02, 03, 05 and 10) where BIOS deposits occurred were the highest in the winter when BIOS seemed to thrive (i.e., thicker deposits). Aluminum and chloride were also both considerably higher in either the winter or spring of 2008, depending on the site.

3.1.3 Geochemical correlations

Non-parametric Spearman rank order correlations were noted to be statistically significant ($p < 0.05$) for a number of geochemical variables (Table 3). In the cases where values were below the limits of detection, half the concentration of the limits of detection for the respective elements was used in the statistical analyses to avoid using zero values. pH and dissolved oxygen were positively correlated ($r_s = 0.44$) while being negatively correlated with dissolved Fe(II) ($r_s = -0.63$ and -0.69, respectively) and DIC ($r_s = -0.64$ and $r_s = -0.61$, respectively). These results agree with the spatial variations observed in Figure 6. DIC was also significantly correlated with DOC ($r_s = 0.33$), $\delta^{13}C_{DIC}$ ($r_s = -0.91$), aluminum ($r_s = 0.38$), magnesium ($r_s = 0.36$), dissolved Fe(II) ($r_s = 0.83$), manganese ($r_s = 0.59$) and chloride ($r_s = 0.52$). Other notable correlations include the expected such as Ca, Mg and Sr, which were all significantly correlated with each other. Manganese was relatively correlated with most of same parameters as those correlated to dissolved Fe(II) with the exception of temperature for which the latter was not significantly correlated.

3.1.4 Predictors of DIC

All geochemical parameters that were significantly correlated with DIC concentrations were computed in step-wise multiple linear regression analyses to determine predicting factors using DIC as the dependent variable. After several steps and removing parameters that did not influence the significance of the model, the final predictors of DIC concentrations included pH, DOC, magnesium, dissolved Fe(II) and chloride (Table 4). The model was strong with 90% of the

variability explained ($R = 0.90$, $p < 2.11E-14$) and all predictors were positively correlated with DIC, with the exception of pH which was negatively correlated.

3.2 Solid phase biogeochemistry

3.2.1 Morphology

Scanning electron microscopy images of BIOS sediments collected at site CR01 in the winter revealed a prolific abundance of tubular sheaths resembling *Leptothrix ochracea*, with occasional helical stalks similar to those produced by *Gallionella ferruginea* (Fig. 1). These microorganisms are known to be Fe(II)-oxidizers and are commonly coated with nano-sized Fe-rich particles (James and Ferris, 2004; Fortin and Langley, 2005; Langley et al., 2009b).

3.2.2 Mineralogy

All BIOS sediment samples analyzed by powder XRD were dominated by 2-line ferrihydrite, as evidenced by two broad peaks at 35° and 60° 2θ, with minor amounts of lepidocrocite (Fig. 7). Trace amounts of goethite were detected in BIOS samples collected at site CR01 in the spring and summer and site CR02 in the spring, summer and fall. On the other hand, the mineralogy of the BIOS at sites CR03 and CR05 did not vary over the seasons. The minerals detected in the sediments of the BIOS-free site were mainly quartz and albite, with minor amounts of microcline and amphibole. These minerals were also found in several of the BIOS samples, as they are the main minerals of the upgradient aquifer material. XRD analysis of the control sample collected in the winter revealed trace amounts of 2-line ferrihydrite; however, the intensity of the peaks was much lower than those observed in other BIOS

sediments. Based on visual field observations, the sediments at the BIOS-free site appeared to have thin layers of iron oxide coatings rather than actual BIOS deposits.

3.2.3 Crystallinity and bioavailability of Fe

The amounts of extractable Fe from BIOS and sediments from the BIOS-free site are shown in Table 5. The extractable Fe using ascorbate may be operationally defined to represent the fraction of bioavailable Fe in the BIOS sediments (Hyacinthe et al., 2006). No seasonal trends were observed in the bioavailability of Fe; however, at site CR02, the fraction of Fe extracted with ascorbate was consistently lower than values observed at the sites nearest to groundwater discharge springs.

The amount of extractable Fe using oxalate was used to determine the amorphous fraction of Fe in the BIOS sediments whereas the difference between the total extractable Fe, using dithionite, and the oxalate extractable Fe represented the crystalline fraction (Table 5). The results indicate that the crystallinity of the reactive Fe in BIOS sediments was generally higher downstream (CR02) than at the groundwater discharge sites (CR01, CR03 and CR05) with the exception of the winter sediments. BIOS closest to groundwater discharge sites had the lowest total sum of extractable Fe in the winter; however, there were no other significant spatial variations.

4. Discussion

4.1 Solid phase biogeochemistry

4.1.1 BIOS occurrence and morphology

Based on visual field observations, groundwater constantly discharged into the wetland while surface water flow rates seemed to be higher in the winter and spring seasons compared to in the summer and fall. The higher flow rates in the spring can be attributed to the snowmelt, which increased surface runoff, whereas in the winter, the higher flow rates was presumably due to either higher water tables, increased surface runoff or less evaporation. Although seasonal variations were observed in the biogeochemistry of the wetland, conditions were consistently suitable for perennial formation and occurrence of BIOS, particularly near the Fe(II)-rich groundwater springs (Fig. 4). BIOS were perennially present within 10 m of groundwater springs; however, there was no macroscopic evidence of Fe(III)-oxide deposition at the control site. The lack of BIOS at the BIOS-free site could either indicate a different source of groundwater that is significantly lower in dissolved Fe(II) concentrations or higher surface water flow rates at the other upstream sites where BIOS form in the wetland. However, some iron oxide coatings were observed at site BF01 in the winter of 2008. It is possible that the site was contaminated or inoculated with FeOB during sampling or simply a random short-term source of dissolved Fe.

The wetland was continually supplied with circumneutral Fe(II)-rich groundwater that discharges at springs where low dissolved oxygen concentrations, low surface water flow rates and low temperatures are observed. These conditions are ideal for the proliferation of FeOB, such as *Gallionella ferruginea* and *Leptothrix ochracea,* thus promoting the continuous

formation and occurrence of BIOS (Andersen and Pedersen, 2003; James and Ferris, 2004; Bruun et al., 2010). BIOS seemed to thrive especially in the winter season, and this may explain the abundance of extracellular structures resembling those produced by *Leptothrix spp. and Gallionella spp.* in the SEM images taken in the winter (Fig. 1). The latter two microorganisms thrived particularly in the winter season when colder temperatures were recorded. In contrast, 16S rRNA analysis of BIOS collected from site CR01 suggested that *Gallionella spp.* was the most dominant microorganism in the winter BIOS, representing nearly 73% of all species detected (Gault et al., 2010 (submitted)). The difference between the results from the microbial analysis and the SEM images may be explained by the fact that *Leptothrix ochracea* has never been isolated and is not represented in molecular biological databases. Also, the tubular sheaths represent biomass and may not necessarily contain any living bacterial cells from which DNA might be extracted. Therefore, *Leptothrix ochracea* is deemed as an unknown species in any genomic analysis, or may not even be detected at all. Other studies have also reported similar SEM observations (James and Ferris, 2004; Langley et al., 2009b). Bruun et al. (2010) mention that tubular structures were observed in their BIOS samples, along with *Gallionella*, which was picked up by molecular analysis. The authors explain that *Leptothrix* was not detected with the molecular analyses because the cells are covered with sheaths that likely protect them during the DNA extraction.

4.1.2 BIOS mineralogy

The Fe(III)-oxide phase that would be expected to precipitate based on the Ostwald step rule, under oxic-anoxic conditions, would be 2-line ferrihydrite, a poorly ordered mineral with

nano-sized particles (Cornell and Schwertmann, 2003). This was confirmed by XRD analysis that revealed 2-line ferrihydrite as the dominant mineral phase in the BIOS sediments. Other studies conducted on the mineralogy of BIOS have also reported 2-line ferrihydrite as the primary mineral phase (Kennedy et al., 2003; Langley et al. 2009b). The trace amounts of lepidocrocite and goethite detected in some of the samples most likely resulted from the dissolution and re-precipitation of 2-line ferrihydrite to form more crystalline iron oxide phases (Cornell and Schwertmann, 2003; Hansel et al., 2003).

Phase transformation of 2-line ferrihydrite is highly dependent on numerous factors, including the role of bacteria-mineral interactions (Kennedy et al., 2004), dissolved Fe(II) concentration, and types of anionic ligands (Cl^-, SO_4^{-2}, CO_3^{-2}) present in the environment (Hansel et al. 2005). The close association of the bacterial cells and exopolymers with the iron oxide particles in the BIOS composite have been shown to increase the phase stability of 2-line ferrihydrite, thus limiting crystallinity transformation (Kennedy et al., 2004). The lack of bacteria in synthetic abiotic ferrihydrite is hypothesized to enhance the Brownian motion of nanoparticles that results in the rearrangement and aggregation of ferrihydrite into more crystalline forms (Penn and Banfield, 1999; Banfield et al. 2000; Kennedy et al. 2004). This bacteria-mineral interaction exists in the BIOS composite and may explain the persistence of nano-sized particles of 2-line ferrihydrite in our samples that did not transform into lepidocrocite and goethite.

The pathways leading to the formation of lepidocrocite and goethite by means of reductive dissolution of 2-line ferrihydrite have been attributed to prevailing concentrations of dissolved Fe(II) (Hansel et al., 2003). At high concentrations of dissolved Fe(II) (> 200 μM),

Hansel et al. (2005) reported that goethite and magnetite were the main secondary mineral phases, while lepidocrocite and goethite dominated at lower dissolved Fe(II) concentrations (< 200 μM). The measured concentrations of dissolved Fe(II) at our study site fell below the 200 μM threshold which is consistent with the lack of magnetite and the presence of trace amounts of lepidocrocite and sometimes goethite in our samples. Technically, goethite should be detected in samples whether the concentration of dissolved Fe(II) was higher or lower than the 200 μM threshold; however, it appeared only as trace amounts in our samples. The open system conditions of the study site mostly likely inhibited the complete phase transformation of 2-line ferrihydrite to lepidocrocite and, finally, to goethite.

Although it may be difficult to compare our results to those from laboratory studies (often representing closed systems), goethite was not detected in the BIOS samples at both sites CR01 and CR02 collected in the winter when the chloride concentrations were high (Table 2). Higher chloride concentrations have been shown to reduce the rate of precipitation of goethite while still precipitating lepidocrocite (Hansel et al., 2005).

4.1.3 BIOS crystallinity and Fe bioavailability

Chemical extractions revealed spatial variations in the crystallinity of BIOS; i.e., downstream BIOS were more crystalline than those nearest to groundwater springs with the exception of the winter samples. This was also reflected in the XRD diffraction patterns where more-ordered Fe(III)-oxide mineral phases, such as lepidocrocite and goethite were more clearly identified in the BIOS sediments from site CR02, when compared to site CR01 (Fig. 7). In addition, the ascorbate-extractable "bioavailable" Fe decreased downstream, concomitant with

an increase in the crystallinity of BIOS, suggesting that the microbial reduction of Fe(III)-oxides at sites downstream was proceeding (Urrutia et al., 1998). The increased crystallinity of such BIOS, via aging or compaction effects, thus makes them less susceptible to microbial Fe(III)-reduction than the freshly precipitated BIOS closest to the groundwater discharge springs. This also indicates that sorbed contaminants would be less likely to be released into solution as a result of reduction of BIOS. However, a recent study by Langley et al. (2009c) found that BIOS underwent complete reductive dissolution in the presence of the model Fe(III)-reducing bacterium *Shewanella putrefaciens* CN32 and that all pre-sorbed Sr was released back into solution. The conditions of that particular study did not take into account the potential re-oxidation of soluble ferrous iron, subsequent hydrolysis and potential re-sorption of mobilized contaminants that may occur across sharp redox gradients typical of our site.

4.2 Aqueous geochemistry

4.2.1 Spatial variations

Several geochemical parameters displayed obvious spatial and seasonal variations throughout the groundwater-supplied wetland (Fig. 6). Near groundwater discharge areas, measured pH values were close to meteoric water values (≈ 5.7) and increased downstream. This trend was also observed for dissolved oxygen concentrations and $\delta^{13}C_{DIC}$ values, which were supported by analyses of nonparametric Spearman rank correlation, where both parameters were positively correlated with pH (r_s= 0.44 and r_s= 0.71, respectively). Both, dissolved Fe(II) and DIC concentrations were negatively correlated with each of the previous three geochemical parameters (Table 3), while displaying inverse spatial trends (Fig. 6). The

increase in dissolved oxygen concentrations downstream from groundwater discharge areas was likely the result of atmospheric oxygen diffusing into the stream water, which may explain the rapid decrease in dissolved Fe(II) concentrations. These observations parallel the results from a different study in a small creek near Deep River, Ontario, Canada, where pH, dissolved oxygen and dissolved Fe(II) concentrations behaved, spatially, in a similar manner (James and Ferris, 2004). However, the spatial scale of our study was much larger, covering an area approximately 12 000 m^2. The aqueous geochemical conditions observed further downstream were more related to typical surface stream water environments (i.e., more dilute and oxygenated conditions than the groundwater that discharged in the wetland). In addition, the low concentrations of dissolved oxygen measured in the warmer summer months (Table 1) were mostly due to the increase of primary productivity in the wetland (Fig. 4), as new organic matter (e.g. leaf litter or branches) was being oxidized. Emerson and Weiss (2004) observed similar seasonal variations in the concentrations of dissolved oxygen in a BIOS-rich freshwater wetland.

The rapid decrease in dissolved Fe(II) concentrations was expected, as the environmental conditions at oxic-anoxic interfaces (i.e., circumneutral pH, low pO_2 and low water flow rates), promote the rapid oxidation of Fe^{2+} to Fe^{3+} (Neubauer et al., 2002). This reaction is typically followed by precipitation of amorphous or poorly-ordered Fe(III)-oxide minerals (Ferris, 2005). These sub-oxic conditions persist all year-round at groundwater discharge areas, which allow FeOB, such as *Gallionella ferruginea* and *Leptothrix ochracea,* to kinetically compete with the rapid chemical oxidation of dissolved Fe(II) by oxygen at circumneutral pH (Neubauer et al., 2002). In addition, pH was generally lower in the winter

months, when BIOS seemed to thrive. This may be explained by the fact that the formation of iron oxides tends to generate more acidity in the solution (Ferris, 2005). Higher redox potential values of the surface water (Table 1), as well as abundant FeOB (Fig. 1) observed in the winter also support the observation that BIOS seemed healthier. In summary, dissolved oxygen concentrations, pH and FeOB are deemed to be important factors in the formation and occurrence of BIOS in this wetland. These geochemical conditions explain the significant amounts of BIOS deposits that occur perennially throughout the wetland, particularly within the first few meters of Fe(II)-rich groundwater springs.

The spatial variations in DIC concentrations and $\delta^{13}C_{DIC}$ values were consistent with CO_2 degassing. In fact, the partial CO_2 pressure calculated for sites near the groundwater springs were greater than the atmospheric pressure (pCO_2 = 0.035 atm) (Table 1). In addition, a study by Doctor et al. (2008) suggests that DIC concentrations are usually higher in the early spring (snowmelt) when compared to values measured in the summer. Those findings agree well with our seasonal DIC concentrations as well as with the depleted $\delta^{13}C_{DIC}$ values measured near the groundwater discharge areas. Although CO_2 degassing may be considered the determining factor in the fate of DIC concentrations and $\delta^{13}C_{DIC}$ values measured downstream from the groundwater discharge areas, BIOS may also play an important role in the biogeochemical cycling of carbon, among other elements. In fact, dissolved Fe(II) and DIC concentrations were positively correlated (r_s = 0.83) suggesting that the two parameters could influence the fate of one another.

4.2.2 Sources and cycles of Fe and DIC

The source of Fe and DIC arise from numerous processes, both chemical and microbial, that naturally occur in the environment. At our study site, the mineralogy of the aquifer deposits, i.e., 10 ka aeolian sand, was mainly composed of silicate minerals, such as quartz, albite, microcline, as well as Fe(II)-bearing minerals (e.g. hornblende), as confirmed by powder X-ray diffraction, EXAFS and petrographic analyses of sediment core samples collected from the wetland. According to Bowen's reaction series, many silicate minerals bearing Fe(II) and Mg that were formed at high crystallization rates tend to be highly susceptible to chemical weathering (see Appendix B). Chemical weathering of silicate minerals is usually induced by the interaction with protons (H^+) present in the groundwater. Rainwater can infiltrate into the aquifer, supplying dissolved atmospheric CO_2 and forming carbonic acid. Subsequently, the dissociation of the latter product generates bicarbonate and releases protons into the groundwater. Upon interaction between Fe(II)-bearing silicate minerals and the slightly acidic groundwater, cations from the minerals, such as Fe^{2+} (as well as other cations, such as Ca^{2+} and Mg^{2+}) are released into solution. This chemical weathering process will ultimately control the total concentration of DIC as well as dissolved Fe(II).

Another important source of both dissolved Fe(II) and DIC includes the microbial reductive dissolution of Fe(III)-oxides, under anaerobic conditions. This process usually occurs at depth, in sediments where Fe(III)-oxides (they may also occur as coatings on sediments such as quartz grains) have been buried over time. Fe(III)-reducing bacteria (e.g., *Geobacter* spp. or *Shewanella* spp.), some of which may be facultative or strict anaerobes, essentially use Fe(III) as the terminal electron acceptor during the oxidation of organic matter and generate alkalinity as

a by-product (Stumm and Morgan, 1996). Such reactions therefore generate additional dissolved Fe(II) and DIC in the groundwater. Measured concentrations of these two geochemical parameters near the groundwater discharge areas support the assumption that extensive chemical weathering of Fe(II)-bearing silicates and, possibly, reductive dissolution of Fe(III)-oxides, are occurring within the upgradient aquifer.

Essentially, the significant correlation between DIC and dissolved Fe(II) in the wetland may be explained by a series of geochemical reactions including the weathering of silicates and, chemosynthesis and precipitation during BIOS formation. The first reaction would be the chemical weathering of a Fe(II)-bearing silicate (almandine (garnet) is used as an example below) by carbonic acid:

$$Fe_3Al_2(SiO_4)_3 + 12CO_2 + 12H_2O \rightarrow 3Fe^{2+} + 2Al^{3+} + 3H_4SiO_4 + 12HCO_3^- \quad \textbf{[5]}$$

The second reaction involves the FeOB, which use chemosynthesis to oxidize Fe(II) to Fe(III) while generating biomass:

$$HCO_3^- + 4Fe^{2+} + 5H^+ \rightarrow CH_2O + 4Fe^{3+} + 2H_2O \quad \textbf{[6]}$$

Finally, the precipitation of Fe(III)-oxides (BIOS) would be the last reaction:

$$Fe^{3+} + 3H_2O \rightarrow Fe(OH)_3 + 3H^+ \quad \textbf{[7]}$$

The overall coupled reactions is therefore:

$$4Fe_3Al_2(SiO_4)_3 + 48CO_2 + 42H_2O + 15H^+ \rightarrow 3CH_2O + 12Fe^{3+} + 8Al^{3+} + 12H_4SiO_4 + 45HCO_3^- \quad \textbf{[8]}$$

This overall process of BIOS formation coupled with the silicate weathering consume generous amounts of dissolved Fe(II) and act as a sink for CO_2. According to the Le Châtelier-Braun principle, if CO_2 is constantly converted into HCO_3^- during BIOS chemosynthesis, then it would lead to increased capture of atmospheric CO_2. In such case, the BIOS deposits would serve as a potential sink for CO_2. However, the DIC concentrations were significantly lower downstream than near the groundwater springs and the calculate pCO_2 values indicate that CO_2 degassing also played a part in the spatial variations observed for DIC and $\delta^{13}C_{DIC}$ values (Table1, Fig. 6).

4.2.3 Geochemical interactions

According to the non-parametric Spearman rank correlation analyses of the geochemical parameters measured at our study site, it is apparent that many parameters are closely linked (Table 3). Given the fact that BIOS deposits may significantly impact the biogeochemical cycling of C in the wetland, it was deemed necessary to statistically assess the geochemical parameters that were significantly correlated with DIC concentrations ($p < 0.05$). These parameters were computed with a statistical software used to run step-wise multi-linear regressions in order to determine the predictors of DIC (dependent variable). Parameters that were not proven to be significant predictors were omitted from future regressions. The final results of the regression analysis yielded five geochemical parameters (i.e., pH, DOC, Mg, Fe(II) and Cl), as the main significant predictors of DIC concentrations in the wetland (Table 4). pH was a variable that greatly influenced the total concentration and speciation of DIC; i.e., if pH increased then the total DIC would also increase (Table 3, Fig. 6). Dissolved Mg and Fe(II) were both likely products of the chemical weathering of silicate minerals such as, biotite [$K(Mg, Fe)_2$

$AlSi_3O_{10}(F, OH)_2]$ or hornblende $[Ca_2(Mg, Fe, Al)_5 (Al, Si)_8O_{22} (OH)_2]$, which both contain the two metals. DOC was also considered a predictor probably because various reactions that often generate or consume DIC in the wetland are indirectly linked to organic matter cycling. Finally, Cl was deemed a predictor as well; however, it is possible that the strong correlation between Cl and DIC was a mere coincidence since the source of Cl remains unknown. One possible explanation would be infiltration of road salt that was used for maintenance of roads nearby the study site. Other parameters (i.e., Al, dissolved oxygen, electrical conductivity, $\delta^{13}C_{DIC}$ and Mn) were significantly correlated with DIC but they did not have a significant influence on the regression model, therefore, they were not considered as valid predictors.

5. Conclusions

The present study was done in a partnership with Atomic Energy of Canada Limited (AECL), located in Chalk River, Ontario, Canada, in order to assess the solid and aqueous phase geochemistry of BIOS deposits forming on their property. The major conclusions drawn from this thesis are the following:

1) The mineralogy of BIOS consisted predominately of amorphous and 2-line ferrihydrite with trace amounts of lepidocrocite. In the warmer months, goethite was occasionally detected at two of the sampled sites (CR01 and CR02). The presence of goethite in some BIOS samples collected downstream suggested that phase transformation processes, such as, reductive dissolution and re-precipitation of more crystalline Fe(III)-oxide phases occurred.

2) Solid phase Fe extractions performed on BIOS deposits revealed that the crystallinity of the Fe was generally higher downstream (CR02) than near the groundwater discharge areas (CR01, CR03 and CR05). In contrast, the bioavailability of Fe decreased as a function of distance from the discharge areas. This suggests that higher crystallinity of BIOS and lower bioavailability of Fe would make BIOS less susceptible to microbial reductive dissolution downstream, thus increasing their redox stability. It may be arguably a short distance between sites CR01 and CR02 (approximately 10 m) to analyse spatial variations, nonetheless, changes in the crystallinity and bioavailability were clearly observed.

3) Spatial trends in a wide range of geochemical parameters were observed throughout the wetland. Statistically significant correlations were also noticed. pH, dissolved oxygen concentrations and $\delta^{13}C_{DIC}$ values, all increased as a function of distance from groundwater discharge areas. These three parameters were positively correlated with each other, while they each were negatively correlated with both dissolved Fe(II) and DIC concentrations. The latter two parameters decreased downstream of discharge areas. Rapid microbial and chemical oxidation of dissolved Fe(II) in a sub-oxic and circumneutral environment resulted in macroscopic deposits of BIOS at the surface of the wetland (within 10 m of groundwater discharge areas). The variations in the DIC and $\delta^{13}C_{DIC}$ values are consistent with CO_2 degassing; however, chemosynthesis used by FeOB during formation of BIOS may also play significant role in the cycling of DIC, thus BIOS acting as a sink for atmospheric CO_2.

6. Environmental implications

The results obtained from this study suggested that the environmental conditions appeared to be consistently suitable for the formation and occurrence of BIOS, particularly near Fe(II)-rich groundwater discharge areas. The fact that the mineralogy of BIOS did not significantly vary over space and time, indicates that BIOS continually have high sorption capacities; i.e., if BIOS tended to undergo more significant phase transformation towards crystalline Fe(III)-oxide phases (e.g., well ordered goethite or hematite), then the surface reactivity would greatly decrease, limiting the availability of sorption sites. The chemical extraction data provided insight into the susceptibility of BIOS reduction by FeRB. Downstream BIOS were less prone to microbial reductive dissolution, thus less likely to release sorbed contaminants back into the environment. Although laboratory studies have suggested that BIOS can undergo complete reduction and dissolution, it remains quite difficult to determine the ultimate fate of BIOS in the natural environment, especially in sub-oxic conditions. Detailed geochemical analyses of the wetland's surface water revealed important geochemical interactions, particularly between dissolved Fe(II) and DIC. The idea that BIOS formation may act as a potential sink for atmospheric CO_2 serves as another potential purpose other than sequestration of dissolved contaminants. However, this concept would require more understanding, thus more field sampling, to determine the precise role of BIOS in the cycling of carbon. BIOS warrant further research in both the laboratory and in the field since they can persist in the environment and potentially provide an inexpensive *in situ* bioremediation approach for contaminated surface and groundwater.

References

Anderson, C.R., James, R.E., Fru, E.C., Kennedy, C.B., Pedersen, K., 2006. In situ ecological development of a bacteriogenic iron oxide-producing microbial community from a subsurface granitic rock environment. Geobiology 4 (1), 29-42.

Anderson, C.R., Pedersen, K., 2003. In situ growth of Gallionella biofilms and partitioning of lanthanides and actinides between biological material and ferric oxyhydroxides. Geobiology 1, 169-178.

Baker, B.J. and Banfield, J.F., 2003. Microbial communities in acid mine drainage. FEMS Microbiol. Ecol. 44, 139-152.

Banfield, J.F., Welsh, S.A., Zhang, H., Ebert, T.T., Penn, R.L., 2000. Aggregation-based crystal growth and microstructure development in natural iron oxyhydroxide biomineralization products. Science 289, 751-754.

Blöthe, M. and Roden, E.E., 2009. Microbial iron redox cycling in a circumneutral-pH groundwater seep. Applied and Environmental Microbiology 75 (2), 468-473.

Bruun, A-M., Finster, K., Gunnlaugsson, H.P., Nørnberg, P., Friedrich, M.W., 2010. A comprehensive investigation on iron cycling in a freshwater seep including microscopy, cultivation and molecular community analysis. Geomicrobiology Journal 27 (1), 15-34.

Châtellier, X., West, M., Rose, J., Fortin, D., Leppard, G., Ferris, F., 2004. Characterization of Iron-Oxides Formed by Oxidation of Ferrous Ions in the Presence of Various Bacterial Species and Inorganic Ligands. Geomicrobiology Journal 21 (2), 99-112.

Cornell, R.M. and Schwertmann, U., 2003. The Iron Oxides: Structure, Properties, Reactions, Occurrence and Uses, 2nd ed. Weinheim, Germany: Wiley-VCH.

Doctor, D.H., Kendall, C., Sebestyen, S.D., Shanley, J.B., Ohte, N., Boyer, E.W., 2008. Carbon isotope fractionation of dissolved inorganic carbon (DIC) due to outgassing of carbon dioxide from a headwater stream. Hydrol. Process. 22, 2410-2423.

Duckworth, O.W., Holmström, S.J.M., Peña, J., Sposito, G., 2009. Biogeochemistry of iron oxidation in a circumneutral freshwater habitat. Chemical Geology 260 (3-4), 149-158.

Edwards, K.J., Rogers, D.R., Wirsen, C.O., McCollom, T.M., 2003. Isolation and characterization of novel psychrophilic, neutrophilic, fe-oxidizing, chemolithoautotrophic α- and γ-Proteobacteria from the deep sea. Applied and Environmental Microbiology 69 (5), 2906-2913.

Edwards, K.J., Bond, P.L., Gihring, T.M., Banfield, J.F., 2000. An archaeal iron-oxidizing extreme acidophile important in acid mine drainage. Science, 287, 1796-1799.

Emerson, D. and Weiss, J.V., 2004. Bacterial iron oxidation in circumneutral freshwater habitats: Findings from the field and the laboratory. Geomicrobiology Journal 21 (6), 405-414.

Emerson, D. and Moyer, C.L., 2002. Neutrophilic Fe-oxidizing bacteria are abundant at the Loihi Seamount hydrothermal vents and play a major role in Fe oxide deposition. Applied and Environmental Microbiology 68 (6), 3085-3093.

Emerson, D., Weiss, J.V., Megonigal, J.P., 1999. Iron-oxidizing bacteria are associated with ferric hydroxide precipitates (Fe-plaque) on the roots of wetland plants. Applied and Environmental Microbiology 65 (6), 2758-2761.

Emerson, D. and Moyer, C., 1997. Isolation and characterization of novel iron-oxidizing bacteria that grow at circumneutral pH. Applied and Environmental Microbiology 63 (12), 4784-4792.

Fein JB, Martin AM and Whightman PG, 1997. Metal adsorption onto bacterial surfaces: development of a predictive approach. Geochim. Cosmochim. Acta, 65, 4267-4273

Ferris, F.G., 2005. Biogeochemical properties of bacteriogenic iron oxides. Geomicrobiology Journal 22 (3-4), 79-85.

Ferris, F.G., Hallberg, R.O., Lyvén, B., Pedersen, K., 2000. Retention of strontium, cesium, lead and uranium by bacterial iron oxides from a subterranean environment. Applied Geochemistry 15 (7), 1035-1042.

Ferris, F.G., Konhauser, K.O., Lyvén, B., Pedersen, K., 1999. Accumulation of metals by bacteriogenic iron oxides in a subterranean environment. Geomicrobiology Journal 16 (2), 181-192.

Fortin, D. and Langley, S., 2005. Formation and occurrence of biogenic iron-rich minerals. Earth Science Reviews 72 (1-2), 1-19.

Fortin, D., Ferris, F.G., Scott, S.D., 1998. Formation of Fe-silicates and Fe-oxides on bacterial surfaces in samples collected near hydrothermal vents on the Southern Explorer Ridge in the northeast Pacific Ocean. Amer. Mineral., 83, 1399-1408.

Fortin, D., Tessier, A. and Leppard, G.G., 1993. Characteristics of lacustrine iron oxyhydroxides. Geochim. Cosmochim. Acta, 57, 4391-4404

Hallbeck, L. and Pedersen, K., 1991. Autotrophic and mixotrophic growth of Gallionella ferruginea. Journal of general microbiology 137 (11), 2657-2661.

Hallberg, R. and Ferris, F.G., 2004. Biomineralization by Gallionella. Geomicrobiology Journal 21 (5), 325-330.

Hansel, C.M., Benner, S.G., Fendorf, S., 2005. Competing Fe(II)-induced mineralization pathways of ferrihydrite. Environmental Science and Technology 39 (18), 7147-7153.

Hansel, C.M., Benner, S.G., Neiss, J., Dohnalkova, A., Kukkadapu, R.K., Fendorf, S., 2003. Secondary mineralization pathways induced by dissimilatory iron reduction of ferrihydrite under advective flow. Geochimica et Cosmochimica Acta 67 (16), 2977-2992.

James, R.E. and Ferris, F.G., 2004. Evidence for microbial-mediated iron oxidation at a neutrophilic groundwater spring. Chemical Geology 212 (3-4 SPEC.ISS.), 301-311.

Kennedy, C.B., Gault, A.G., Clark, I.D., Fortin, D. and Ferris, F.G., 2010. Retention of Iodide by Bacteriogenic Iron Oxides. Geomicrobiology J. (in press)

Kennedy, C.B., Scott, S.D., Ferris, F.G., 2004. Hydrothermal phase stabilization of 2-line ferrihydrite by bacteria. Chemical Geology 212 (3-4 SPEC.ISS.), 269-277.

Kennedy, C.B., Scott, S.D., Ferris, F.G., 2003. Characterizationof bacteriogenic iron oxide deposits from Axial Volcano, Juan de Fuca Ridge, northeast Pacific ocean. Geomicrobiology Journal 20 (3), 199-214.

Kostka, J.E. and Luther III, G.W., 1994. Partitioning and speciation of solid phase iron in saltmarsh sediments. Geochimica et Cosmochimica Acta 58 (7), 1701-1710.

Kulczycki, E., Fowle, D.A., Fortin, D., Ferris, F.G., 2005. Sorption of cadmium and lead by bacteria-ferrihydrite composites. Geomicrobiology Journal 22 (6), 299-310.

Langley, S., Igric, P., Takahashi, Y., Sakai, Y., Fortin, D., Hannington, M.D., Schwarz-Schampera, U., 2009a. Preliminary characterization and biological reduction of putative biogenic iron oxides (BIOS) from the Tonga-Kermadec Arc, southwest Pacific Ocean. Geobiology 7 (1), 35-49.

Langley, S., Gault, A.G., Ibrahim, A., Takahashi, Y., Renaud, R., Fortin, D., Clark, I.D., Ferris, F.G., 2009b. Sorption of strontium onto bacteriogenic iron oxides. Environmental Science and Technology 43 (4), 1008-1014.

Langley, S., Gault, A.G., Ibrahim, A., Takahashi, Y., Renaud, R., Fortin, D., Clark, I.D., Ferris, F.G., 2009c. Strontium desorption from bacteriogenic iron oxides (BIOS) subjected to microbial Fe(III) reduction. Chemical Geology 262 (3-4), 217-228.

Martinez, R.E. and Ferris, F.G., 2005. Review of the surface chemical heterogeneity of bacteriogenic iron oxides: Proton and cadmium sorption. American Journal of Science 305 (6-8 SPEC. ISS.), 854-871.

Martinez, R.E., Smith, D.S., Pedersen, K., Ferris, F.G., 2003. Surface Chemical Heterogeneity of Bacteriogenic Iron Oxides from a Subterranean Environment. Environmental Science and Technology 37 (24), 5671-5677.

Neubauer, S.C., Emerson, D., Megonigal, J.P., 2002. Life at the energetic edge: Kinetics of circumneutral iron oxidation by lithotrophic iron-oxidizing bacteria isolated from the wetland-plant rhizosphere. Applied and Environmental Microbiology 68 (8), 3988-3995.

Nielsen, P., 2004. The biological role of strontium. Bone 35, 583-588.

Ontario wetland evaluation system northern manual (OWES), 2003. Ministry of Natural Resources, Government of Ontario, Canada.

Penn, R.L. and Banfield, J.F., 1999. Morphology development and crystal growth in nanocrystalline aggregates under hydrothermal conditions: insights from titania. Geochim. Cosmoschim. Acta 63, 1549-1557.

Small, T.D., Warren, L.A., Roden, E.E., Ferris, F.G., 1999. Sorption of strontium by bacteria, fe(III) oxide, and bacteria - Fe(III) oxide composites. Environmental Science and Technology 33 (24), 4465-4470.

St-Jean, G., 2003. Automated quantitative and isotopic (13C) analysis of dissolved inorganic carbon and dissolved organic carbon in continuous-flow using a total organic carbon analyser. Rapid Communications in Mass Spectrometry 17 (5), 419-428.

Stookey, L.L., 1970. Ferrozine - A new spectrophotometric reagent for iron. Analytical Chemistry 42 (7), 779-781.

Stumm, W. and Morgan, JJ., 1996. Aquatic Chemistry: Chemical Equilibria and Rates in Natural Waters. John Wiley & Sons, New York.

Warren, L.A. and Ferris, F.G, 1998. Continuum between sorption and precipitation of Fe(III) on microbial surfaces. Environmental Science and Technology 32 (15), 2331-2337.

Weiss, J.V., Rentz, J.A., Plaia, T., Neubauer, S.C., Merrill-Floyd, M., Lilburn, T., Bradburne, C., Megonigal, J.P., Emerson, D., 2007. Characterization of neutrophilic Fe(II)-oxidizing bacteria isolated from the rhizosphere of wetland plants and description of Ferritrophicum radicicola gen. nov. sp. nov., and Sideroxydans paludicola sp. nov. Geomicrobiology Journal 24 (7-8), 559-570.

Figure 1. Scanning electron micrographs showing the microbial morphology associated with surface BIOS sediments collected in the winter 2007 from site CR01. Micrograph (A) shows the dominance of tubular sheaths similar to those of *Leptothrix ochracea* (L) and (B) occasional helical stalks resembling those of *Gallionella ferruginea* (G).

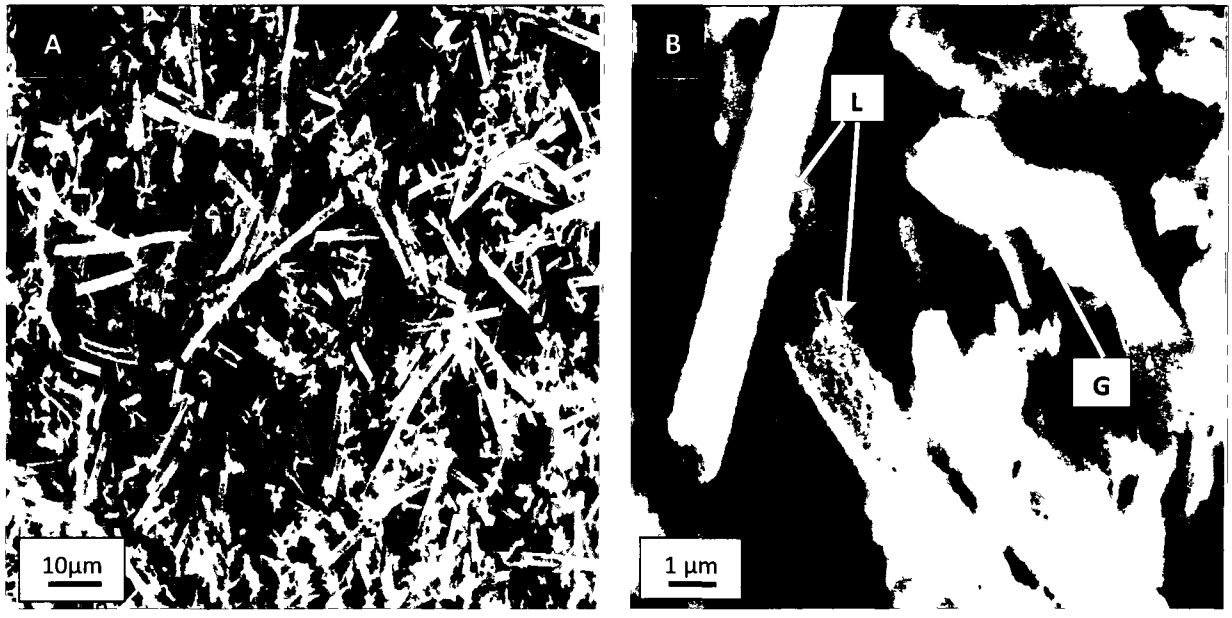

Figure 2. Map of Ontario, Canada with the location of Chalk River with respect to Ottawa and Toronto.

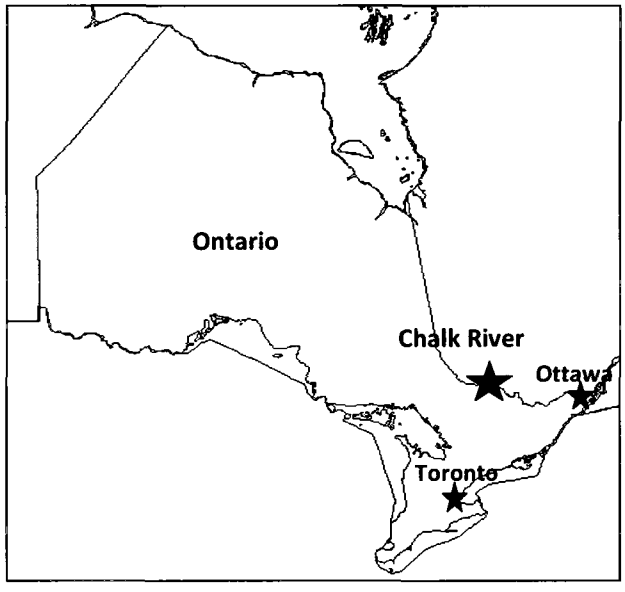

Figure 3. Regional map (Google Earth image) of the location of the study site with respect to recharge zone (Lake 233) and the general groundwater flow path (blue arrow) of the area.

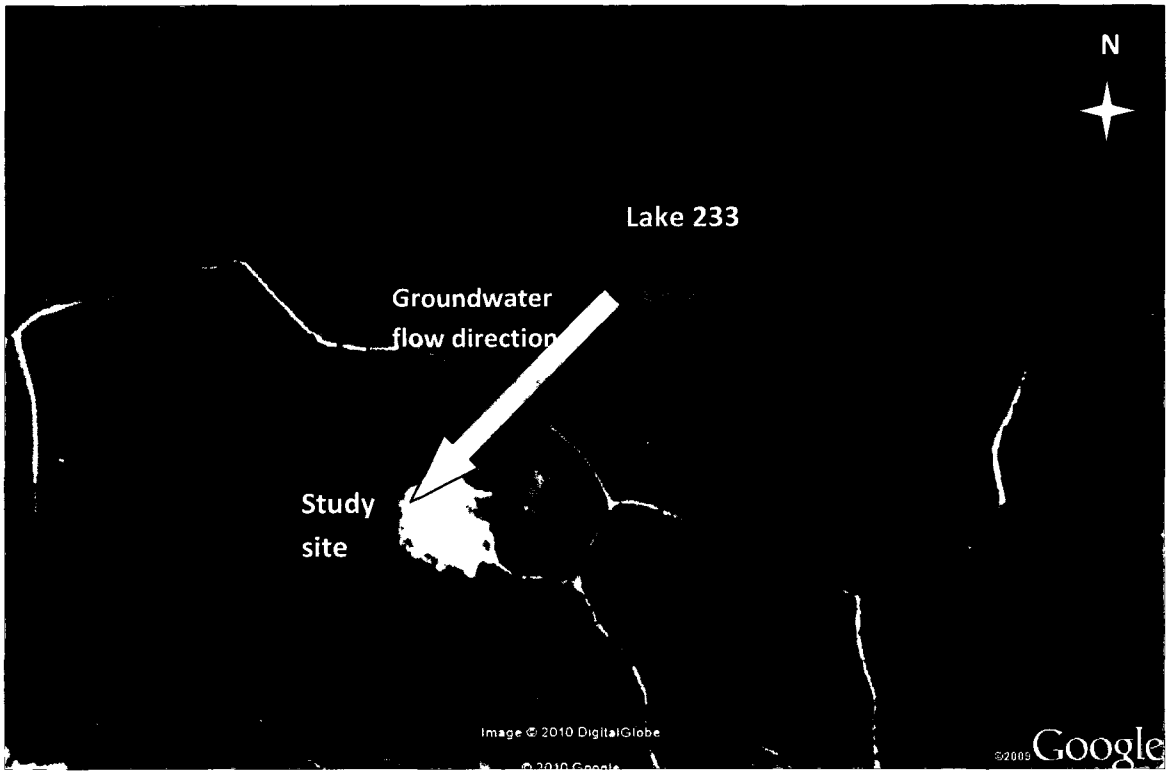

Figure 4. Seasonal photographs of the Fe(II)-rich groundwater discharge area (site CR01), where there is extensive accumulation of BIOS. Photograph (A) was taken in winter 2007, (B) in spring 2008, (C) in summer 2007 and (D) in fall 2007.

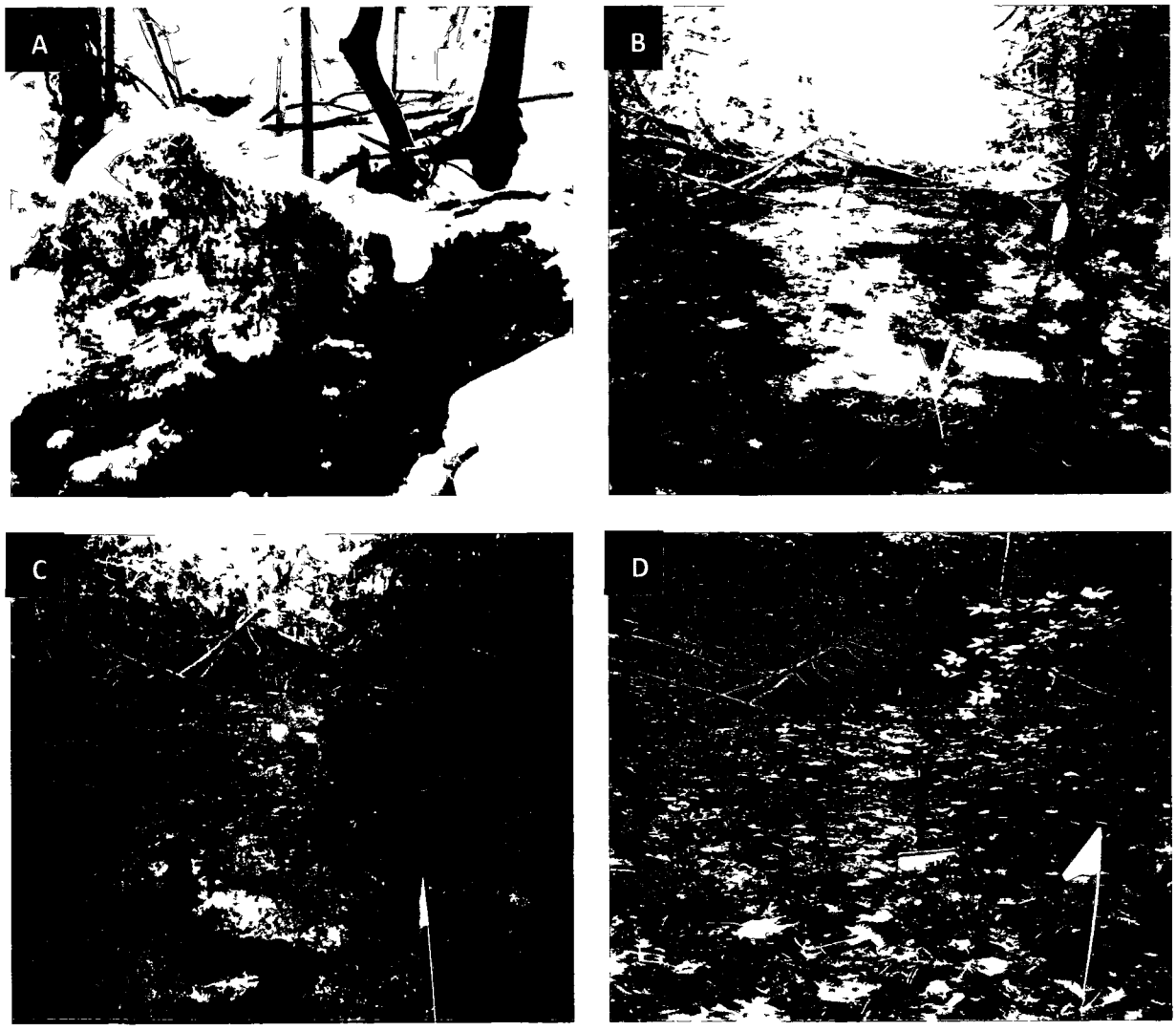

Figure 5. Map with the location of the 11 sampling sites within the wetland boundaries where BIOS formed and occurred. Sampling points were mapped with UTM coordinates.

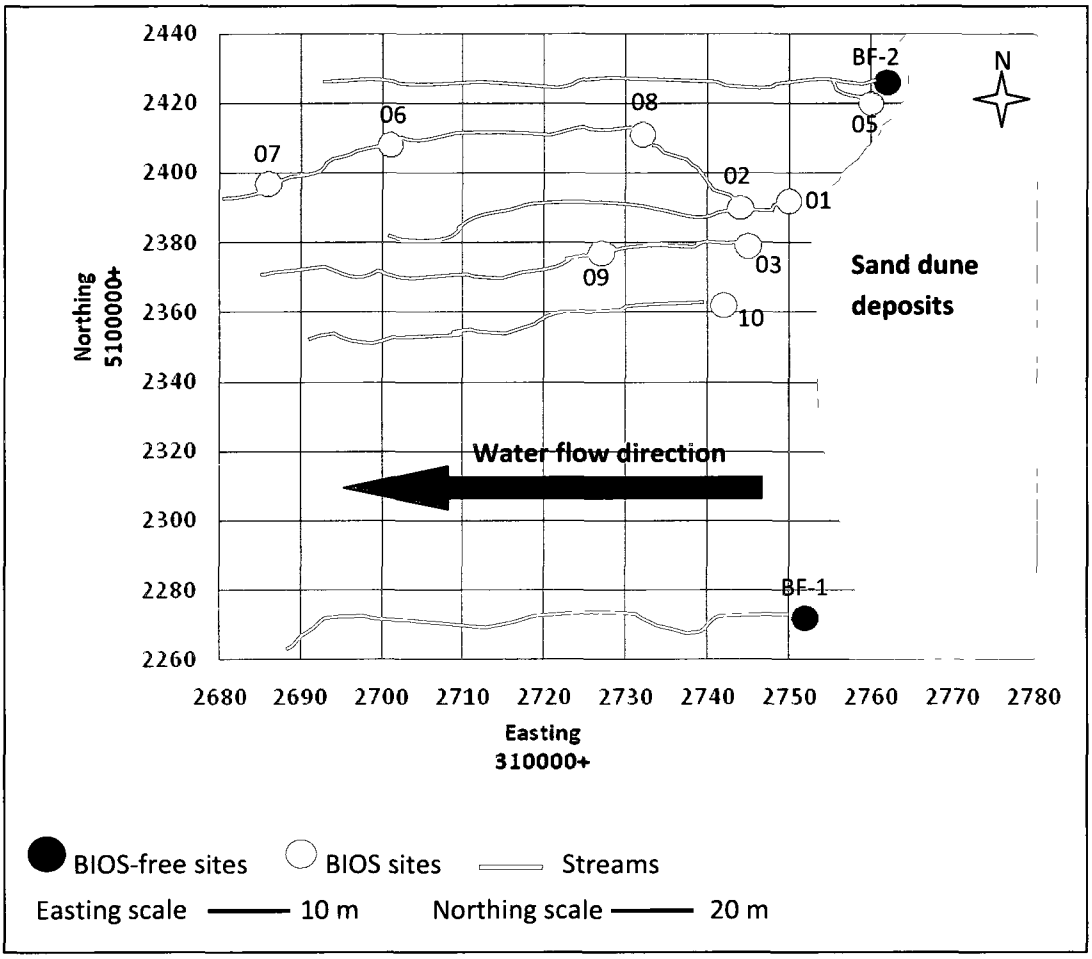

Figure 6. Spatial variations of the physicochemical and geochemical parameters of the surface water in the wetland. Shown are dissolved oxygen, pH, dissolved Fe(II), Fe(III), DIC and $\delta^{13}C_{DIC}$

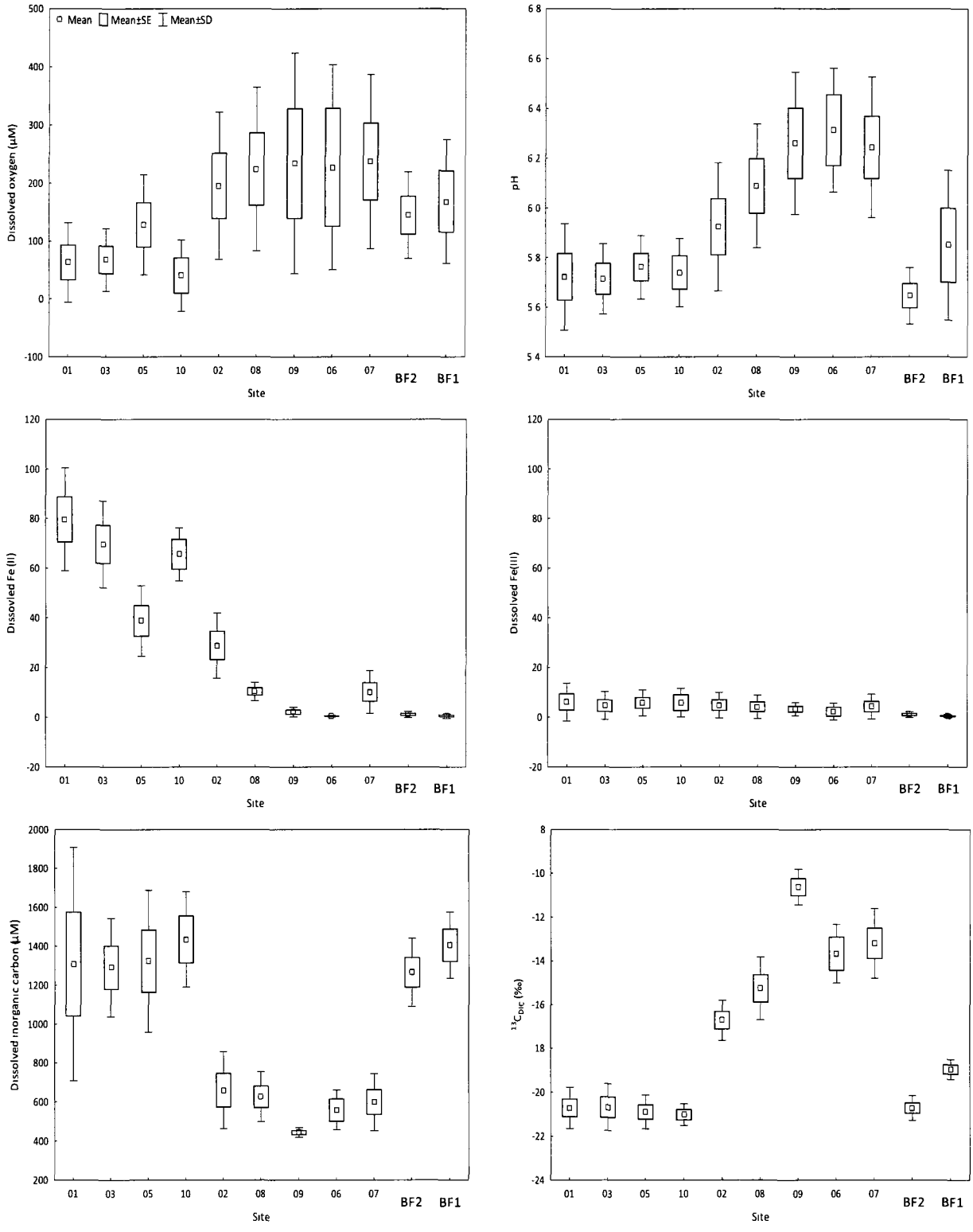

Figure 7. Seasonal X-ray diffraction patterns of surface BIOS and control sediments collected in the spring, summer and fall of 2007 and winter of 2008 from sites CR01, CR02, CR03, CR05 and BIOS-free-1. Ferric iron mineral phases appear as broad peaks (F = 2-line ferrihydrite, L = lepidocrocite, G = goethite, S= sample holder). Sharper peaks corresponded to silicate minerals i.e., Q = quartz, albite, microcline and amphibole.

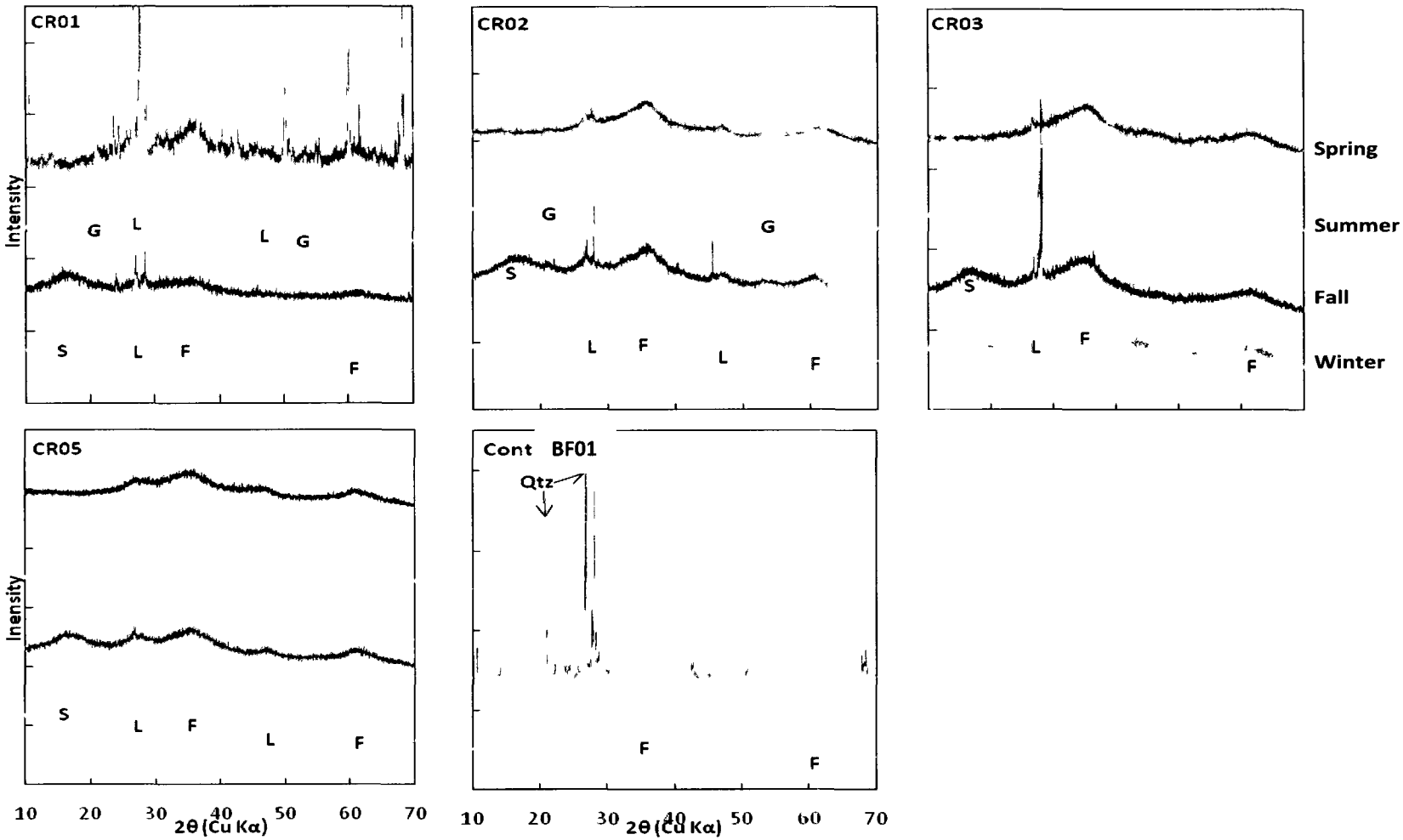

Table 1. Physicochemical parameters of the surface water in the wetland.

Site ID	Season	Site Location[a]	pH	Eh mV)	Temp (°C)	EC (μS/cm)	DO (μM)	DIC (μM)	DOC (μM)	$^{13}C_{DIC}$ (‰)	$^{13}C_{DOC}$ (‰)	pCO_2 (atm)
CR-01	Apr-07	Upstream	6.0	247	8.0	40	155	949	199	-19.4	-26.6	0.012
	Jul-07	Upstream	5.9	212	9.2	34	1.56	819	392	-20.3	-27.3	0.012
	Oct-07	Upstream	5.6	245	9.3	1.0	26.9	1032	475	-21.5	-27.4	0.016
	Feb-08	Upstream	5.5	315	4.0	33	13.8	1440	291	-20.7	-26.3	0.019
	Apr-08	Upstream	5.7	238	7.1	30	117	2298	366	-21.6	-26.7	0.033
CR-02	Apr-07	Midstream	6.1	248	8.4	19	342	672	201	-17.0	-26.2	0.008
	Jul-07	Midstream	6.2	230	10.3	35	26.9	519	274	-15.8	-27.6	0.006
	Oct-07	Midstream	5.8	288	9.6	15	288	504	516	-16.2	-27.7	0.007
	Feb-08	Midstream	5.6	381	3.1	14	200	616	266	-16.5	-26.7	0.008
	Apr-08	Midstream	5.9	241	6.7	20	119	991	291	-18.2	-26.8	0.013
CR-03	Apr-07	Upstream	5.8	237	8.4	46	60.6	1159	233	-20.1	-27.1	0.016
	Jul-07	Upstream	5.7	317	8.9	25	5.63	1156	167	-21.1	-27.5	0.017
	Oct-07	Upstream	5.5	300	8.7	46	28.1	1399	308	-21.8	-27.4	0.022
	Feb-08	Upstream	5.8	302	7.5	38	104	1057	241	-19.1	-26.9	0.014
	Apr-08	Upstream	5.8	277	7.7	41	139	1682	383	-21.2	-26.8	0.023
CR-05	Apr-07	Upstream	5.8	308	8.9	39	239	1040	274	-19.8	-27.1	0.015
	Jul-07	Upstream	5.9	345	9.6	44	9.69	1073	326	-21.3	-27.6	0.015
	Oct-07	Upstream	5.7	284	8.8	45	80.9	1249	400	-21.5	-27.6	0.019
	Feb-08	Upstream	5.6	377	4.2	41	155	1316	325	-20.3	-26.5	0.017
	Apr-08	Upstream	5.9	310	7.1	0.0	156	1940	391	-21.6	-26.8	0.025

Table 1. Cont'd

Site ID	Season	Site Location	pH	Eh (mV)	Temp (°C)	EC (µS/cm)	DO (µM)	DIC (µM)	DOC (µM)	$^{13}C_{DIC}$ (‰)	$^{13}C_{DOC}$ (‰)	pCO_2 (atm)
CR-06	Apr-07	Downstream	6.2	320	7.8	27	373	484	222	-12.2	-27.1	0.005
	Jul-07	Downstream	6.6	289	9.9	34	30.6	518	226	-14.7	-27.4	0.004
	Oct-07	Downstream	6.2	252	10.2	43	278	674	333	-14.2	-27.0	0.008
	Feb-08	Downstream	-[b]	-[b]	-[b]	-[b]	-[b]	-[b]	-[b]	-[b]	-[b]	-[b]
	Apr-08	Downstream	-[b]	-[b]	-[b]	-[b]	-[b]	-[b]	-[b]	-[b]	-[b]	-[b]
CR-07	Apr-07	Downstream	6.2	242	8.6	32	364	434	283	-10.9	-27.5	0.005
	Jul-07	Downstream	6.6	221	11.8	37	30.6	486	207	-12.7	-27.7	0.004
	Oct-07	Downstream	6.2	227	10.0	0.0	327	575	341	-13.5	-27.3	0.006
	Feb-08	Downstream	5.8	288	1.9	14	339	741	241	-15.2	-26.4	0.008
	Apr-08	Downstream	6.3	252	6.0	0.0	125	758	325	-13.8	-27.3	0.007
CR-08	Apr-07	Downstream	6.2	255	6.6	37	331	464	249	-12.9	-26.8	0.005
	Jul-07	Downstream	6.4	236	13.0	42	24.4	534	323	-14.8	-27.5	0.006
	Oct-07	Downstream	6.2	258	9.6	18	283	666	441	-16.1	-27.2	0.008
	Feb-08	Downstream	5.7	333	2.8	18	350	674	258	-16.2	-26.7	0.008
	Apr-08	Downstream	6.1	264	5.4	36	131	791	341	-16.3	-27.2	0.009
CR-09	Apr-07	Downstream	-[b]	-[b]	-[b]	-[b]	-[b]	-[b]	-[b]	-[b]	-[b]	-[b]
	Jul-07	Downstream	6.4	212	12.9	1.0	28.4	460	213	-11.6	-27.5	0.004
	Oct-07	Downstream	6.3	245	9.1	21	352	450	308	-11.0	-27.4	0.004
	Feb-08	Downstream	5.8	336	1.4	24	433	458	258	-10.2	-27.0	0.005
	Apr-08	Downstream	6.5	247	6.3	18	122	408	216	-9.77	-26.1	0.003

Table 1. Cont'd

Site ID	Season	Site Location	pH	Eh (mV)	Temp (°C)	EC (µS/cm)	DO (µM)	DIC (µM)	DOC (µM)	$^{13}C_{DIC}$ (‰)	$^{13}C_{DOC}$ (‰)	pCO_2 (atm)
CR-10	Apr-07	Upstream	-[b]	-[b]	-[b]	-[b]	-[b]	-[b]	-[b]	-[b]	-[b]	-[b]
	Jul-07	Upstream	5.6	270	9.0	32	1.88	1286	251	-21.6	-27.7	0.020
	Oct-07	Upstream	5.8	277	8.6	51	18.1	1241	391	-20.7	-27.4	0.018
	Feb-08	Upstream	5.8	285	8.6	48	8.75	1432	325	-20.6	-27.1	0.021
	Apr-08	Upstream	5.9	267	8.5	26	133	1782	366	-21.2	-26.4	0.024
BF01	Apr-07	Upstream	-[b]	-[b]	-[b]	-[b]	-[b]	-[b]	-[b]	-[b]	-[b]	-[b]
	Jul-07	Upstream	5.4	405	8.9	24	20.3	1201	163	-18.9	-27.3	0.019
	Oct-07	Upstream	6.0	295	8.6	8.0	214	1424	200	-19.6	-27.7	0.019
	Feb-08	Upstream	5.9	336	6.0	40	270	1382	266	-18.5	-26.6	0.017
	Apr-08	Upstream	6.1	332	6.7	21	168	1615	183	-19.0	-26.3	0.018
BF02	Apr-07	Upstream	5.6	245	7.5	21	153	1139	240	-19.9	-26.8	0.017
	Jul-07	Upstream	5.8	335	7.9	31	14.1	1145	215	-21.0	-27.4	0.016
	Oct-07	Upstream	5.5	338	7.6	27	171	1241	233	-21.2	-27.5	0.019
	Feb-08	Upstream	5.6	375	6.9	15	194	1232	200	-20.4	-26.3	0.018
	Apr-08	Upstream	5.7	371	7.3	29	190	1565	233	-21.2	-26.6	0.022

[a] Sites located upstream, midstream and downstream are less than a meter, approximately 10 m and greater than 10 m from the groundwater springs, respectively.

[b] Data not collected

Errors: pH (± 0.2); Eh (± 20 mV); temperature (± 0.15 °C); EC = electrical conductivity (± 0.5% + 1µS/cm); DO =dissolved oxygen (± 6.25 µM); DIC and DOC =dissolved inorganic and organic carbon, respectively (± 2%); $^{13}C_{DIC}$ and $^{13}C_{DOC}$ (±0.2‰)

Table 2. Chemical composition of the surface water in the wetland. All values are μM.

Site ID	Season	Site Location [a]	Al	Na	K	Ca	Mg	Si	Sr	Fe-II	Fe(III)	Mn	Cl	SO_4
		LOQ	0.20	0.20	0.74	0.22	0.03	0.53	0.001	0.30	0.06	0.01	14.1	10.4
CR-01	Apr-07	Upstream	bdl	149	21.7	93.0	59.6	178	0.32	77.7	bdl	1.00	99.2	60.7
	Jul-07	Upstream	1.83	111	19.4	73.1	45.7	183	0.33	56.6	3.92	1.06	33.9	45.8
	Oct-07	Upstream	bdl	105	22.0	79.0	47.5	167	0.40	68.6	8.15	1.33	39.0	14.7
	Feb-08	Upstream	16.3	104	25.1	91.3	57.2	165	0.30	83.1	18.3	1.09	120	37.4
	Apr-08	Upstream	6.67	161	16.6	117	71.6	183	0.40	112	bdl	1.27	224	42.8
CR-02	Apr-07	Midstream	bdl	132	26.7	97.0	61.3	196	0.31	30.7	bdl	0.56	84.3	80.8
	Jul-07	Midstream	0.72	134	17.6	87.6	54.8	198	0.33	8.06	4.28	1.12	49.4	60.4
	Oct-07	Midstream	bdl	122	28.3	93.1	54.1	174	0.32	31.9	8.39	1.37	39.7	24.9
	Feb-08	Midstream	11.5	113	26.9	97.1	58.4	171	0.27	28.8	11.7	0.73	105	81.7
	Apr-08	Midstream	53.7	165	22.3	115	67.9	187	0.35	44.6	bdl	0.73	188	41.7
CR-03	Apr-07	Upstream	bdl	190	22.8	100	64.2	222	0.39	74.3	bdl	1.58	97.1	83.3
	Jul-07	Upstream	0.72	164	23.0	111	70.0	219	0.45	80.6	2.49	1.99	113	84.3
	Oct-07	Upstream	bdl	173	29.0	111	68.5	222	0.42	83.6	7.78	2.03	54.1	43.1
	Feb-08	Upstream	2.37	154	23.5	100	62.1	211	0.35	39.8	12.8	1.46	142	32.6
	Apr-08	Upstream	1.15	217	14.8	98.6	62.5	211	0.39	69.2	0.07	1.64	123	79.4
CR-05	Apr-07	Upstream	bdl	118	24.1	137	90.7	197	0.50	46.9	bdl	0.86	147	69.5
	Jul-07	Upstream	1.09	87.0	22.0	124	76.6	198	0.45	44.9	1.95	0.90	84.6	59.3
	Oct-07	Upstream	bdl	133	26.5	134	77.9	188	0.49	43.7	5.62	1.33	59.7	27.7
	Feb-08	Upstream	6.30	119	26.3	138	83.9	182	0.47	13.6	13.1	0.73	161	88.4
	Apr-08	Upstream	10.8	130	30.9	195	118	201	0.68	44.7	8.27	0.91	242	200

Table 2. Cont'd.

Site ID	Season	Site Location [a]	Al	Na	K	Ca	Mg	Si	Sr	Fe-II	Fe(III)	Mn	Cl	SO_4
CR-06	Apr-07	Downstream	bdl	83.5	22.8	112	60.3	214	0.46	0.20	0.64	0.13	25.0	46.2
	Jul-07	Downstream	0.35	85.7	16.6	116	62.6	212	0.45	0.39	bdl	0.15	-[b]	-[b]
	Oct-07	Downstream	bdl	98.5	26.8	154	82.8	226	0.58	0.75	6.18	0.81	26.2	27.3
	Feb-08	Downstream	-[b]	-[b]	-[b]	-[b]	-[b]	-[b]	-[b]	-[b]	-[b]	-[b]	-[b]	-[b]
	Apr-08	Downstream	-[b]	-[b]	-[b]	-[b]	-[b]	-[b]	-[b]	-[b]	-[b]	-[b]	-[b]	-[b]
CR-07	Apr-07	Downstream	bdl	90.2	23.9	107	59.3	216	0.42	1.80	1.06	0.15	30.6	51.6
	Jul-07	Downstream	0.24	94.4	16.9	118	65.0	215	0.45	2.15	0.88	0.22	-[b]	-[b]
	Oct-07	Downstream	bdl	108	25.9	131	75.8	226	0.48	8.85	9.88	0.70	31.4	30.7
	Feb-08	Downstream	19.3	111	27.6	110	65.8	206	0.38	16.9	9.73	0.53	108	53.2
	Apr-08	Downstream	4.82	109	25.3	122	70.8	212	0.43	20.8	bdl	0.51	102	61.0
CR-08	Apr-07	Downstream	bdl	140	23.0	97.0	62.1	204	0.35	5.90	1.38	0.35	98.6	71.8
	Jul-07	Downstream	0.35	107	22.3	114	72.0	215	0.45	9.13	1.41	0.46	-[b]	-[b]
	Oct-07	Downstream	bdl	124	24.6	112	68.8	202	0.40	13.2	6.86	0.67	43.9	25.0
	Feb-08	Downstream	5.26	132	22.5	98.6	58.4	186	0.32	8.47	11.0	0.73	139	44.3
	Apr-08	Downstream	3.48	152	13.6	110	67.1	187	0.38	15.0	0.06	0.47	196	48.2
CR-09	Apr-07	Downstream	-[b]	-[b]	-[b]	-[b]	-[b]	-[b]	-[b]	-[b]	-[b]	-[b]	-[b]	-[b]
	Jul-07	Downstream	0.35	160	24.8	120	75.7	212	0.45	3.94	2.67	1.44	-[b]	-[b]
	Oct-07	Downstream	bdl	165	26.9	122	75.2	213	0.60	0.75	5.69	1.86	49.7	40.0
	Feb-08	Downstream	4.71	153	25.1	110	64.2	199	0.35	bdl	5.01	0.51	105	72.9
	Apr-08	Downstream	0.44	183	14.3	102	65.0	203	0.40	3.62	bdl	0.73	143	73.6

Table 2. Cont'd.

Site ID	Season	Site Location [a]	Al	Na	K	Ca	Mg	Si	Sr	Fe-II	Fe(III)	Mn	Cl	SO_4
CR-10	Apr-07	Upstream	-[b]	-[b]	-[b]	-[b]	-[b]	-[b]	-[b]	-[b]	-[b]	-[b]	-[b]	-[b]
	Jul-07	Upstream	-[b]	-[b]	-[b]	-[b]	-[b]	-[b]	-[b]	-[b]	-[b]	-[b]	-[b]	-[b]
	Oct-07	Upstream	bdl	166	29.3	125	72.5	192	0.49	58.7	6.20	1.76	83.6	22.7
	Feb-08	Upstream	7.78	162	29.7	124	67.5	183	0.42	60.2	11.5	1.64	183	37.7
	Apr-08	Upstream	47.4	183	35.5	140	74.9	183	0.50	77.9	bdl	2.00	241	36.0
BF01	Apr-07	Upstream	-[b]	-[b]	-[b]	-[b]	-[b]	-[b]	-[b]	-[b]	-[b]	-[b]	-[b]	-[b]
	Jul-07	Upstream	0.31	89.6	21.5	187	102	258	0.67	bdl	bdl	0.04	81.8	41.6
	Oct-07	Upstream	bdl	97.7	23.1	191	102	263	0.60	bdl	0.45	0.08	49.6	18.8
	Feb-08	Upstream	27.1	96.6	26.6	176	97.1	257	0.58	bdl	1.43	0.09	126	37.3
	Apr-08	Upstream	2.97	113	22.8	177	96.7	255	0.82	1.77	0.02	0.46	307	44.3
BF02	Apr-07	Upstream	bdl	86.6	19.4	109	57.0	218	0.45	0.70	0.63	0.18	35.6	73.3
	Jul-07	Upstream	0.35	79.6	17.1	114	60.1	212	0.45	2.15	0.16	0.26	31.0	35.4
	Oct-07	Upstream	bdl	103	18.4	107	54.8	215	0.43	bdl	2.86	0.24	12.7	18.2
	Feb-08	Upstream	3.60	76.6	22.0	106	53.9	206	0.40	bdl	1.79	0.18	28.5	45.8
	Apr-08	Upstream	79.0	117	8.95	109	55.9	206	0.45	2.72	bdl	0.25	32.1	51.0

[a] Sites located upstream, midstream and downstream are less than a meter, approximately 10 m and greater than 10 m from groundwater springs, respectively.

[b] Data not collected

bdl = below detection limits; LOQ = limit of quantification (μM)

Table 3. Spearman rank correlation coefficients of the physicochemical and geochemical parameters.

	pH	Eh	Temp	EC	DO	DIC	DOC	$^{13}C_{DIC}$	$^{13}C_{DOC}$	Al	Na	K	Ca	Mg	Si	Sr	Fe(II)	Fe(III)	Mn	Cl	SO4
pH	1.00																				
Eh	**-0.46**	1.00																			
Temp	0.19	**-0.38**	1.00																		
EC	-0.30	0.07	0.20	1.00																	
DO	**0.44**	0.10	-0.24	**-0.42**	1.00																
DIC	**-0.64**	0.20	-0.04	**0.41**	**-0.61**	1.00															
DOC	-0.13	-0.14	**0.39**	-0.01	-0.22	**0.33**	1.00														
$^{13}C_{DIC}$	**0.71**	-0.18	-0.14	**-0.36**	**0.66**	**-0.91**	**-0.40**	1.00													
$^{13}C_{DOC}$	-0.06	0.15	**-0.69**	-0.18	0.25	0.12	**-0.40**	0.07	1.00												
Al	-0.26	0.30	**-0.60**	-0.22	-0.20	**0.38**	0.00	-0.20	**0.51**	1.00											
Na	-0.13	-0.16	-0.14	0.29	-0.24	0.29	-0.12	-0.22	0.16	0.09	1.00										
K	-0.15	0.32	0.06	-0.07	0.19	0.14	0.19	-0.08	0.02	0.04	-0.04	1.00									
Ca	0.08	0.20	0.12	0.14	0.07	0.32	0.27	-0.14	-0.05	0.09	0.01	**0.47**	1.00								
Mg	0.05	0.15	0.14	0.18	-0.01	**0.36**	0.24	-0.22	-0.04	0.03	0.12	**0.36**	**0.94**	1.00							
Si	**0.45**	-0.16	0.21	0.05	0.24	-0.27	-0.27	**0.36**	-0.24	**-0.40**	0.06	0.03	0.27	0.30	1.00						
Sr	0.16	0.03	**0.34**	0.16	0.00	0.24	0.30	-0.14	-0.28	-0.19	0.00	**0.35**	**0.86**	**0.82**	**0.41**	1.00					
Fe(II)	**-0.63**	0.00	0.09	0.30	**-0.69**	**0.83**	0.19	**-0.87**	0.03	0.20	**0.33**	0.01	-0.05	0.04	**-0.34**	-0.04	1.00				
Fe(III)	**-0.42**	**0.45**	-0.02	-0.08	-0.02	0.06	0.22	-0.08	-0.05	0.17	-0.30	**0.45**	-0.02	-0.08	-0.16	-0.08	-0.10	1.00			
Mn	**-0.47**	-0.02	**0.39**	**0.39**	**-0.60**	**0.59**	0.26	**-0.65**	-0.24	-0.02	**0.55**	0.21	0.06	0.12	-0.11	0.20	**0.68**	0.13	1.00		
Cl	-0.28	0.30	**-0.60**	0.00	-0.18	**0.52**	-0.12	**-0.33**	**0.57**	**0.73**	**0.46**	-0.04	0.23	0.28	**-0.35**	-0.01	**0.35**	-0.11	0.12	1.00	
SO4	0.06	0.23	**-0.44**	-0.05	0.12	-0.02	**-0.55**	0.07	**0.34**	0.21	0.13	-0.21	-0.09	0.03	0.16	-0.11	-0.05	-0.30	-0.26	**0.35**	1.00

Value in bold indicates correlation coefficients that are significantly correlated ($p < 0.05$)

Table 4. Multiple regression analysis used to determine significant predictors of dissolved inorganic carbon (dependent variable). $R^2 = 0.90$, n= 36, F = 54.2, $p < 0.05$

Independent Variables	Parameter estimates	DIC Std. Error	p-value	Mean	Std. Dev	Beta coefficient (β)
pH	-110.5	27.6	0.000	5.90	0.30	-0.608
DOC	0.95	0.35	0.011	312	79.0	0.283
Mg	10.8	2.41	0.000	67.8	12.9	0.693
Fe(II)	9.84	0.96	0.000	38.2	31.1	0.449
Cl	2.08	0.54	0.001	106	62.2	0.236

Table 5. Seasonal measurements of extractable solid phase Fe from surface BIOS and BIOS-free sediments using four non-sequential chemical extractants. Also shown are the fractions of the bioavailable Fe, the amorphous and crystalline iron oxide phases.

Site	Season	Solid phase Fe ($mg\ g^{-1}$)				Bioavailable Fe	Crystallinity Of Fe	
		HCl	Ascorbate (A)	Oxalate (O)	Dithionite (D)		Amor.	Cryst.
		($mg\ g^{-1}$)				%	%	
						A/D	O/D	(D-O)/D
CR01	**Spring**	23.6	22.2	46.8	47.2	47.0	99.0	1.0
	Summer	23.6	20.1	37.3	41.5	48.5	89.9	10.1
	Fall	27.0	29.5	49.7	52.8	55.9	94.2	5.8
	Winter	13.1	12.1	14.5	19.8	61.2	73.3	26.7
CR02	**Spring**	28.0	23.9	44.1	66.6	35.9	66.2	33.8
	Summer	22.2	16.7	48.3	58.4	28.7	82.8	17.2
	Fall	13.8	12.9	36.5	47.6	27.0	76.6	23.4
	Winter	29.5	14.4	42.4	53.2	27.1	79.6	20.4
CR03	**Spring**	38.7	33.1	48.8	49.4	67.1	98.7	1.3
	Summer	33.3	32.4	50.2	62.5	51.8	80.4	19.6
	Fall	18.6	19.0	25.9	24.5	77.6	100.0+	0.0
	Winter	12.9	14.9	18.0	21.9	67.9	82.0	18.0
CR05	**Spring**	31.9	27.5	36.1	42.2	65.3	85.5	14.5
	Summer	32.4	38.2	48.7	49.8	76.7	97.8	2.2
	Fall	31.4	25.5	35.3	34.7	73.3	100.0+	0.0
	Winter	7.36	7.02	6.25	8.64	81.3	72.3	27.7
BF01	**Spring**	-[a]	-[a]	-[a]	-[a]	-[a]	-[a]	-[a]
	Summer	0.03	0.41	2.19	2.17	18.9	100.0+	0.0
	Fall	0.54	0.96	1.80	1.88	50.8	95.6	4.4
	Winter	16.4	8.61	26.5	19.2	45.0	100.0+	0.0

[a] Data not collected

Amor. = Amorphous; Cryst. = Crystalline

Errors are presented in Appendix A

Appendix A

Errors for the solid phase Fe extractions

		Solid phase Fe (mg g^{-1})			
Site	**Season**	**HCl**	**Ascorbate (A)**	**Oxalate (O)**	**Dithionite (D)**
CR01	**Spring**	1.84	3.47	8.09	3.23
	Summer	3.70	6.78	2.95	0.18
	Fall	0.30	1.01	4.07	0.15
	Winter	1.33	1.27	2.13	0.60
CR02	**Spring**	1.52	0.75	4.51	0.18
	Summer	2.11	2.14	3.69	0.45
	Fall	1.38	6.40	3.97	9.90
	Winter	1.96	0.44	3.85	3.96
CR03	**Spring**	1.68	1.79	10.41	0.64
	Summer	1.80	0.90	4.70	0.63
	Fall	0.45	1.34	1.47	0.49
	Winter	0.84	1.49	0.96	1.28
CR05	**Spring**	15.47	0.06	7.14	0.06
	Summer	1.20	1.03	0.68	3.16
	Fall	2.39	0.85	0.04	1.83
	Winter	0.64	0.72	0.40	0.35
BF01	**Spring**	-[a]	-[a]	-[a]	-[a]
	Summer	0.04	0.10	0.30	0.16
	Fall	0.01	0.45	0.25	0.11
	Winter	1.20	0.63	3.16	0.54

[a] Data not collected

Amor. = Amorphous; Cryst. = Crystalline

Appendix B

Bowen's reaction series